ITEK8-29949 FR2

A31274-1 GW

1 APRIL 1976

SQT

VOLUME IIA (2)

PLANETARY CAMERA FINAL REPORT

SPACE TELESCOPE OPTICAL TELESCOPE ASSEMBLY/SCIENTIFIC INSTRUMENTS PHASE B PRELIMINARY DESIGN AND PROGRAM DEFINITION STUDY

(NASA-CR-150118) SPACE TELESCOPE OPTICAL TELESCOPE ASSEMBLY/SCIENTIFIC INSTRUMENTS. PHASE B: -PRELIMINARY DESIGN AND PROGRAM DEFINITION STUDY; VOLUME 2A: PLANETARY CAMERA REPORT Final Report (Itek Corp.)

N77-14844 HC A03 MF A01

Unclas G3/74 58344

Prepared for
GEORGE C. MARSHALL SPACE FLIGHT CENTER
NATIONAL AERONAUTICS AND SPACE ADMINISTRATION
MARSHALL SPACE FLIGHT CENTER, ALABAMA

Under contract NAS8-29949

GODDARD SPACE FLIGHT CENTER
NATIONAL AERONAUTICS AND SPACE ADMINISTRATION
GREENBELT, MARYLAND

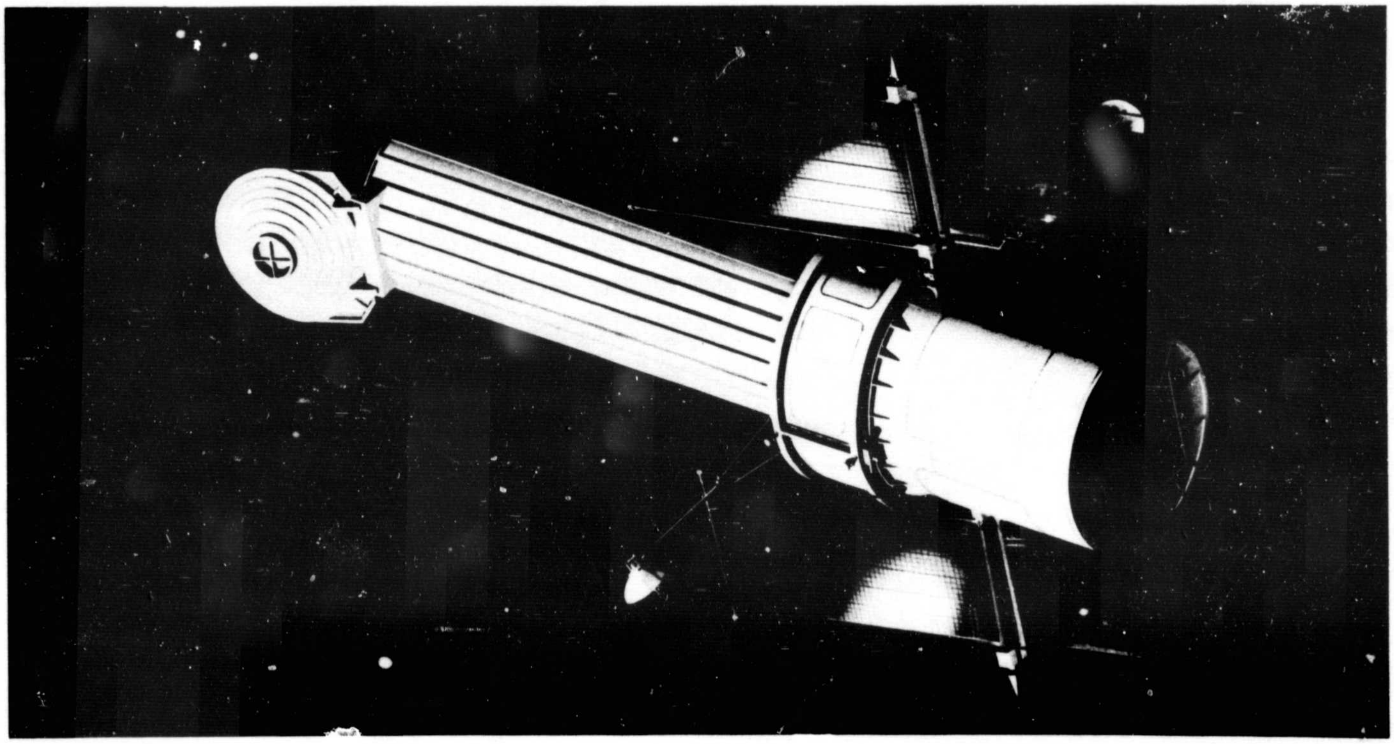

Itek
Optical Systems
A Division of Itek Corporation
10 Maguire Road
Lexington, Massachusetts 02173

Bendix
Aerospace Systems Division

MARTIN MARIETTA
DENVER DIVISION

Lockheed
MISSILES & SPACE COMPANY, INC.

VOLUME IIA (2)

PLANETARY CAMERA FINAL REPORT

ITEK

CONTENTS PAGE

1.0 INSTRUMENT CHARACTERISTICS

Table 1.1 lists the F/48, F/96 Planetary Camera characteristics as taken from the SI Requirements Document, LST Scientific Instrument Requirements for Preliminary Design, revised 15 April 1975 (Goddard Space Flight Center). Additional requirements are taken from the Final Instrument Definition, LST High Resolution Camera (HRC FID) by the Imaging Instrument Definition Team.

TABLE 1.1

INSTRUMENT CHARACTERISTICS

DETECTOR	CCD
Photocathode	-
Window	Silicon Chip
Cooling	-40°C
Data Format	9.2 x 9.2 MM
Resolution	15 Lp/MM
ACQUISITION	Spacecraft
Positional Accuracy	1 Arcsec
STABILITY	± .007 Arcsec
CALIBRATION	
Internal	Tungsten Lamp
External	Standard Stars
FIELD-OF-VIEW	F/48 17 x 17 Arcsec
	F/96 8 x 8 Arcsec
ANGULAR RESOLUTION	0.1 Arcsec F/48
	Diff. Limited F/96
RANGE	180 - 1200 NM
EXPOSURE TIME	10 Msec - 5 Min
FILTERS	28

Table 1.2 summarizes the Itek design to meet the requirements of Table 1.1. The Planetary Camera has an optical system with two, selectable focal lengths imaging on a CCD detector cooled to -40°C. The optical system consists of two independent, two-mirror relays nested together in such a way as to have two separate entrance apertures in the OTA focal plane and a common output focal plane. Switching between the relays is accomplished by means of the multi-position capping shutter.

The camera also includes a filter assembly consisting of 28 filters in four coaxial wheels.

The detector can be calibrated by flooding the detector face with light, either from a standard star or from an internal source. The standard star calibration system has separate, two-mirror optical system with its own entrance aperture. The internal calibration source illuminates the detector directly. No additional moving parts are required by the calibration system.

The detector requires an exposure control shutter. This is integrated into the detector assembly in order to maximize shutter efficiency.

The average power is 64 watts. The weight is estimated to be 218 pounds.

TABLE 1.2

PLANETARY CAMERA

Nested Two-Mirror Relays With Common Output

- 4:1 for F/96 - Diffraction-Limited Image
- 2:1 for F/48 - Near-Diffraction-Limited Image

CCD Detector Cooled to -40°C

28 Filters in Four-Wheel Assembly

Detector Calibration System With No Moving Parts

- Calibration with Standard Stars
- Calibration with Internal Source

Exposure Control Shutter

Capping Shutter

Average Power - 64 Watts

Weight - 218 Pounds

2.0 LAYOUT

The layout for the Planetary Camera is shown in Figure 2.1.

The F/48, F/96 Planetary Camera consists of two relays at 2:1 and 4:1 magnification, a CCD Camera submodule and electronics, filter assembly, standard star calibration system, internal source calibration system, and capping shutter assembly. These components are mounted on an invar optical bench which is connected to the instrument housing at the three instrument support points.

The optical bench has a forward bay for the optics which is enclosed with a thermal shroud whose temperature is thermostatically controlled. The optical bench also has an aft bay for the detector. This bay has built into it a thermal reflector to increase the view factor of the camera submodule to the outer wall of the instrument housing.

Figure 2.2 shows a schematic of the calibration system as it fits in with the relay optics. Two options are allowed as either the light from internal sources or standard stars may be used. For standard star calibration, the capping shutter is positioned to close the entrance apertures to the relays but open the entrance aperture to the calibration system. The light from a star enters this aperture, is reflected by a fold mirror, and then is diverged, rather than imaged, by a diverging mirror so that the detector is flooded. The field lens forms a pupil image at the detector. The image is off-center so that image of the obscuration does not fall upon the detector. The standard star calibration system uses a separate entrance aperture in the OTA focal plane. It contains two mirrors, the first one flat, the second, a weak sphere, which allow the beam to expand to about four times the size of the detector surface. A quartz field lens near the entrance aperture forms an image of the primary mirror at the detector. The image is off-center enough so that the detector surface fits in the area between the central obscuration image and the edge.

For internal source calibration, the capping shutter blocks all entrance apertures. One of several calibration sources located as shown, is used to illuminate the focal plane. Silicon diode detectors are used to monitor the output of the calibration sources.

The capping shutter has four positions, admitting light into the F/48 relay, the F/96 relay, or the standard star calibration system, or capping all optical paths.

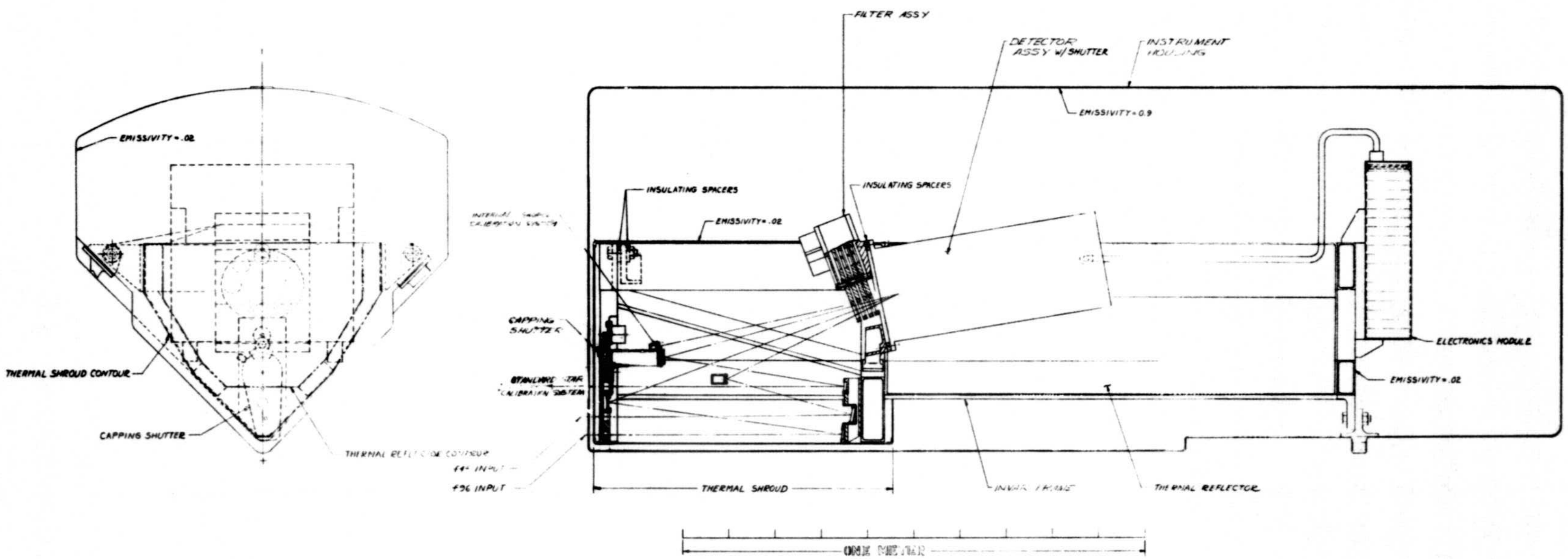

FIGURE 2.1

F/48, F/96 PLANETARY CAMERA LAYOUT

FIGURE 2.2 CALIBRATION SYSTEM SCHEMATIC

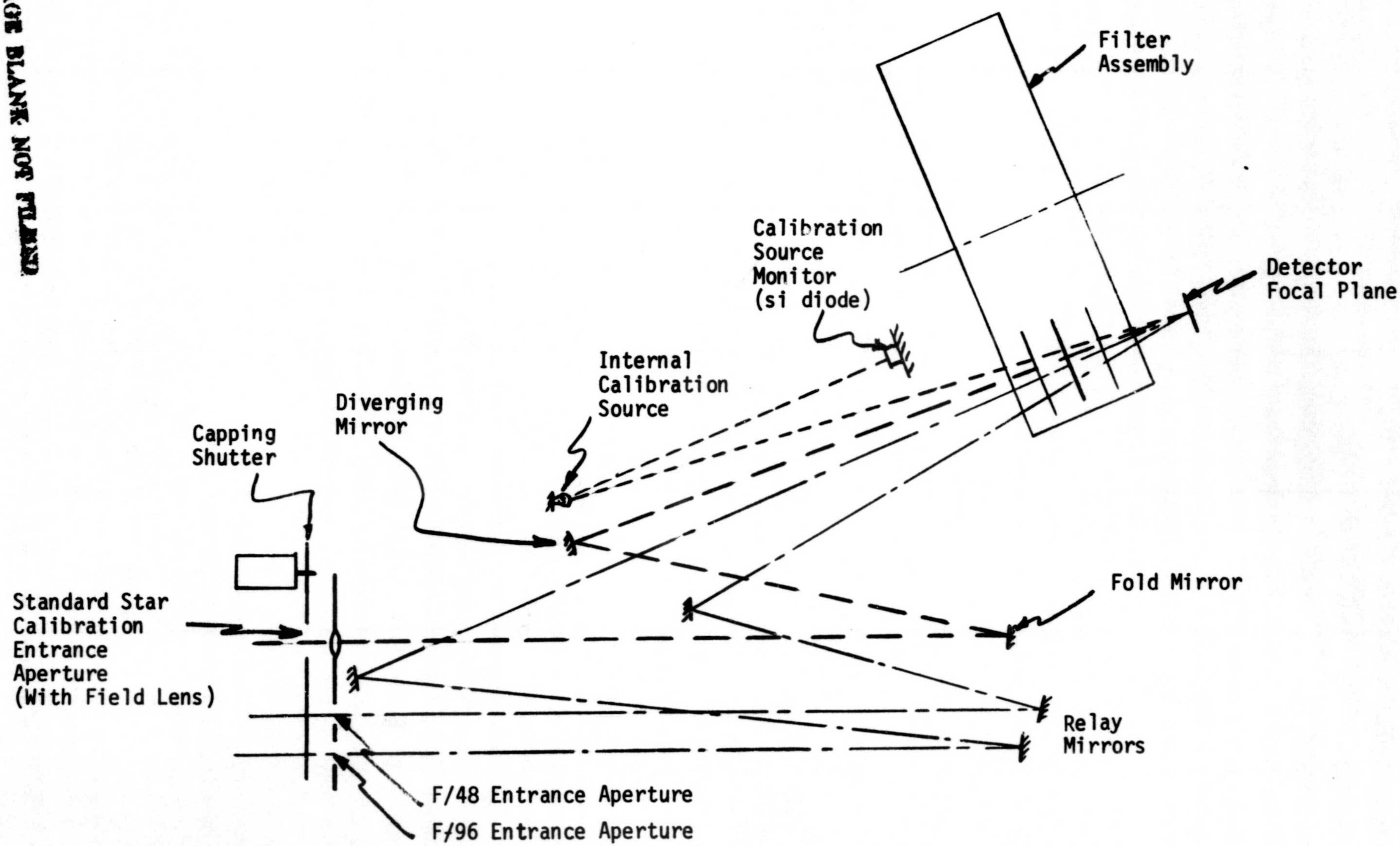

PRECEDING PAGE BLANK NOT FILMED

3.0 OPTICAL DESIGN

The relays of the Planetary Camera are two-mirror eccentric systems with an unvignetted output format of 9.2 mm square. The F/96 relay gives virtually diffraction-limited performance over the entire field, while the F/48 relay gives near-diffraction-limited performance.

Figure 3.1 shows the relay design. The input aperture for the F/48 relay is centered 92.1 mm off the OTA axis, while the input aperture for the F/96 relay is centered 54.1 mm off the OTA axis. The common output focal plane lies 629.5 mm behind the OTA focal plane vertex and is centered 358.5 mm off the OTA axis. It is tipped 5.4 degrees from normal to that axis. The size of the output focal plane is 9.2 x 9.2 mm square.

The computer ray trace spot diagrams for the F/96 relay are shown in Figure 3.2 for the center field position and at positions around the periphery of the 10 x 10 mm field at the output of the relay. Only half the image plane is shown because of the left-right symmetry with respect to the center of the format. Note that the scale of the individual spot diagrams is different from the image plane scale.

At F/96, the airy disc diameter at 0.325 micrometer wavelength is 76 micrometers. The worst case spot diagrams for the relay show geometric image spread of less than 5 micrometers diameter. Hence, the relay can be considered virtually diffraction-limited. The departure of the best-fit spherical focal surface from flat over the field of the relay is negligible.

Figure 3.3 shows the spot diagrams for the F/48 relay. The worst-case geometric spread falls within a 10 micrometer circle. As the airy disc diameter at 0.325 micrometer wavelength is 36 micrometers, this relay can be considered nearly diffraction-limited also.

Alignment sensitivity calculations for the relays were not made, but the sensitivities should not be vastly different than those computed for an F/24 relay of similar dimensions. For that relay, image growth of around 1.5 micrometer could be expected from mirror misalignments of 0.1 mm and 0.1 milliradian. One might expect the same order of magnitude image growth for the F/48 and F/96 relays, reflected to the F/24 input focal plane. At the F/96 output focal plane, the corresponding image growth would be 6 micrometers, which would considerably enlarge the original geometric spot, but if the tolerances are reduced by a factor of three, then undergraded performance can be expected. This is the basis of the tolerances given in Figure 3.4.

FIGURE 3.1

F/48, 96 PLANETARY CAMERA RELAY

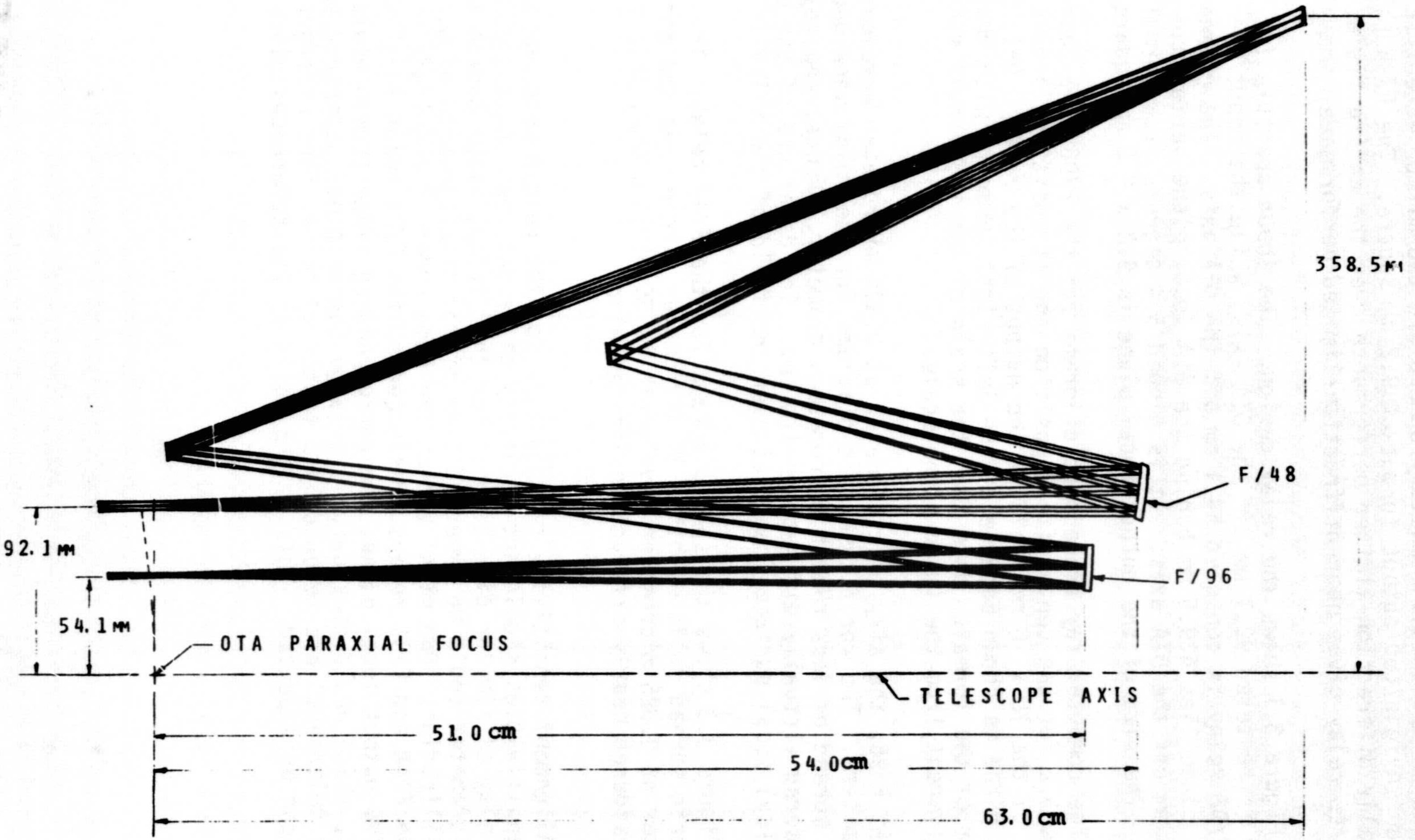

SCHU1724 OPTICSG8 18H52M18 75.149

FIGURE 3.2
F/96 RELAY IMAGES

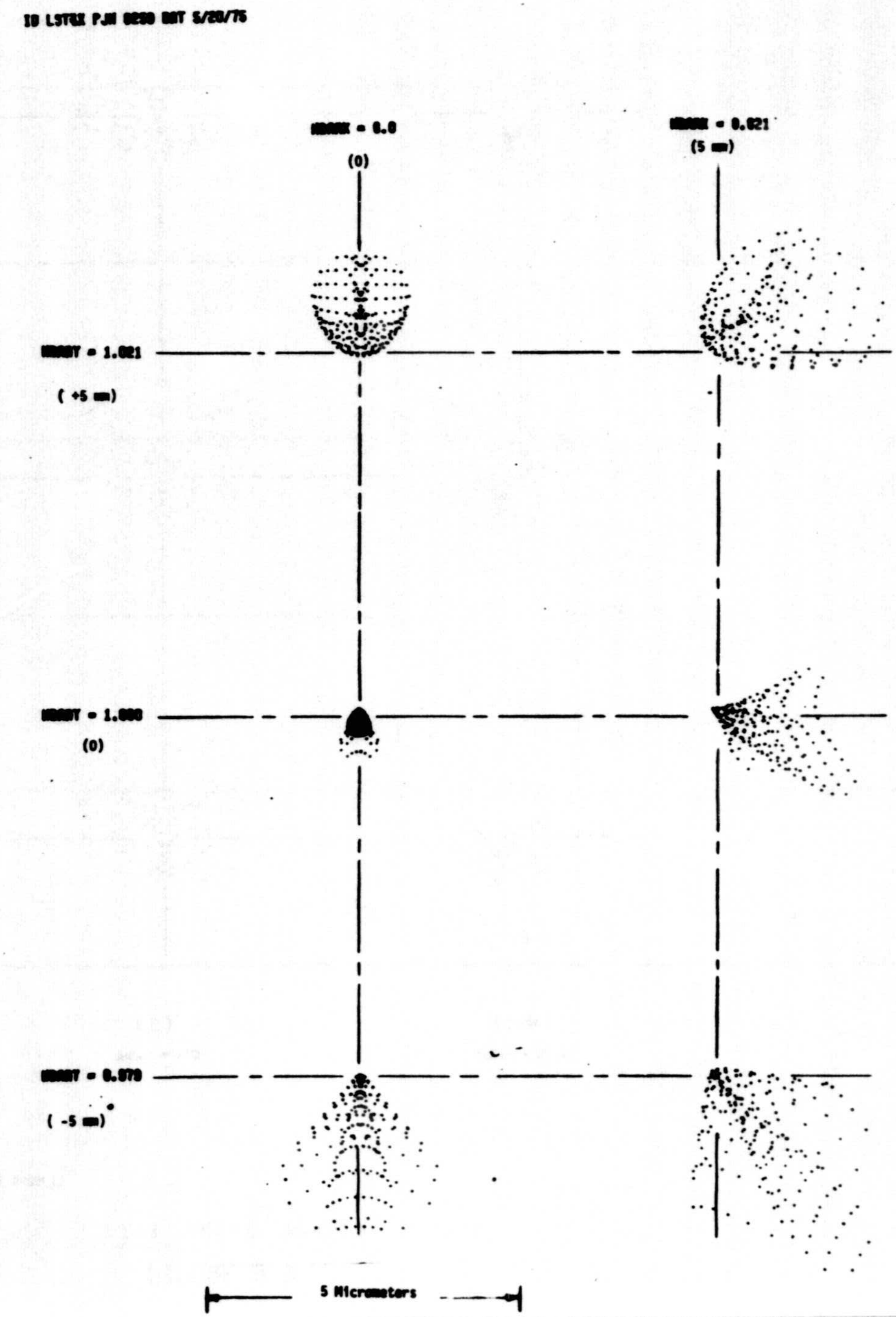

FIGURE 3.3

F/48 RELAY IMAGES

ID LST2X PJN 0250 DAT 5/20/75

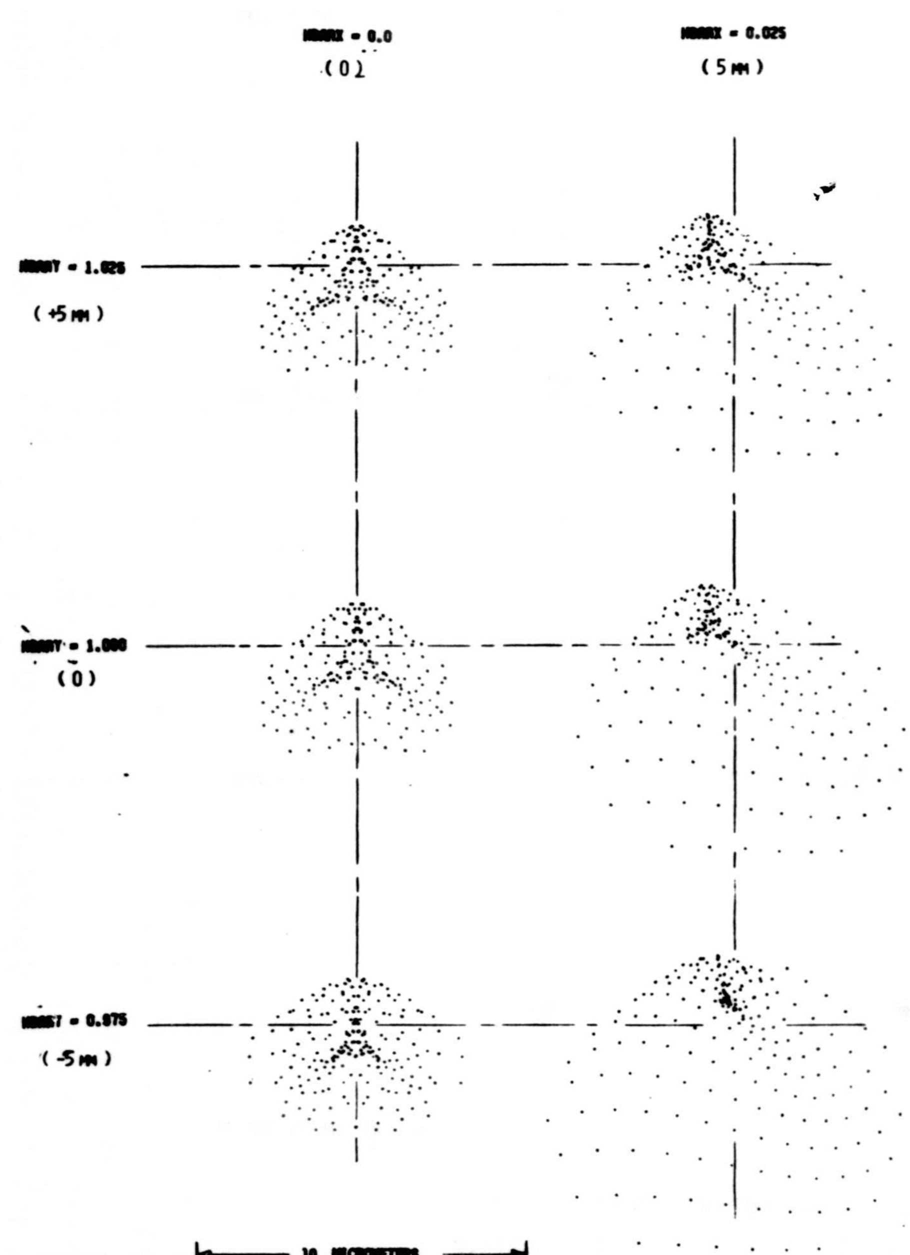

FIGURE 3.4

ALIGNMENT TOLERANCES FOR

F/48, 96 PLANETARY CAMERA

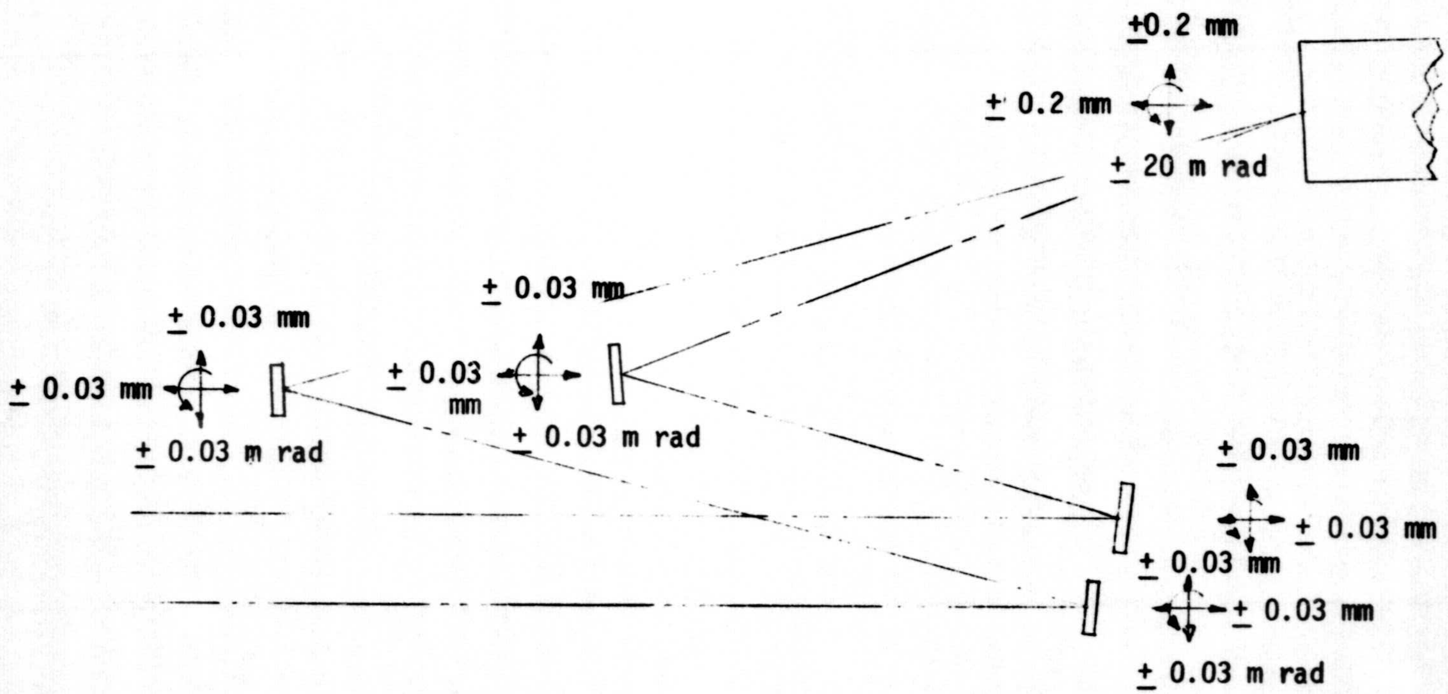

4.0 CCD CAMERA SUBMODULE THERMAL DESIGN

No attempt was made to produce a layout drawing of what the CCD Camera submodule would actually look like, but thermal analysis of the cooling of the detector was carried far enough to provide a preliminary estimate of the cooling power required and the submodule size required for dissipation of the heat generated within the submodule.

A detector similar to that in the JPL Prototype 400 x 400 array CCD Camera was assumed. Thermoelectric cooling of the detector was provided. Heat dissipation by radiation from the submodule walls was assumed. The total power was estimated to be within the 30 watts peak power defined in the SI Requirements Document.

The configuration assumed for thermal analysis is shown in Figure 4.1. The detector, whose total size is about 3 inches long by 1 inch wide by 1/4 inch thick, is mounted to a cold plate. The cold plate, in turn, is mounted on three thermoelectric coolers, which are mounted to a heat sink at 300°K (80°F). The coolers are similar to Cambion Model 801-1004 two-stage coolers.

The detector is to be cooled to 230°K (-45°F). Its front face is covered by a thermal blanket except for the part immediately in front of the detector area. The sides of the detector are unshielded thermally, and radiate with an emissivity of 0.2 to the 300°K environment.

The largest heat leak to the detector is through the leads. To minimize this, connectors are placed on the cold plate with the detector to mate with the detector terminals. From the connectors, on each side of the detector, a mylar film with electroplated copper leads 0.001 inch thick by 0.025 inch wide by 0.5 inch long bridges to a terminal adjacent to the driver electronics, mounted on the heat sink. It is assumed that there are, in all, 24 of the copper leads. With leads of this type, it may be necessary to limit the data rates from the chip to 100 Khz to avoid problems of lead inductance and cross-coupling, but this presents no problem since the camera is used in a snapshot mode.

The CCD detector cooling is accomplished with three thermoelectric coolers similar to the Cambion Model 801-1004 two-stage cooler. The cooler electronics will drive each cooler at 6 amperes. Under this condition, the electrical power dissipated in each cooler is 16 watts, and the cooling capacity is a simple linear function of the temperature difference across the cooler through which the heat must be pumped, as shown in Figure 4.2.

The results of the thermal analysis indicate that about 0.75 watt must be pumped by the cooler. The largest heat source is the leak through the leads, about 0.63 watt. The radiative leak into the detector is about 0.075 watt, while the electrical power dissipated directly within the chip can be expected to be on the order of 0.05 watt.

FIGURE 4.1

COOLING OF CCD DETECTOR

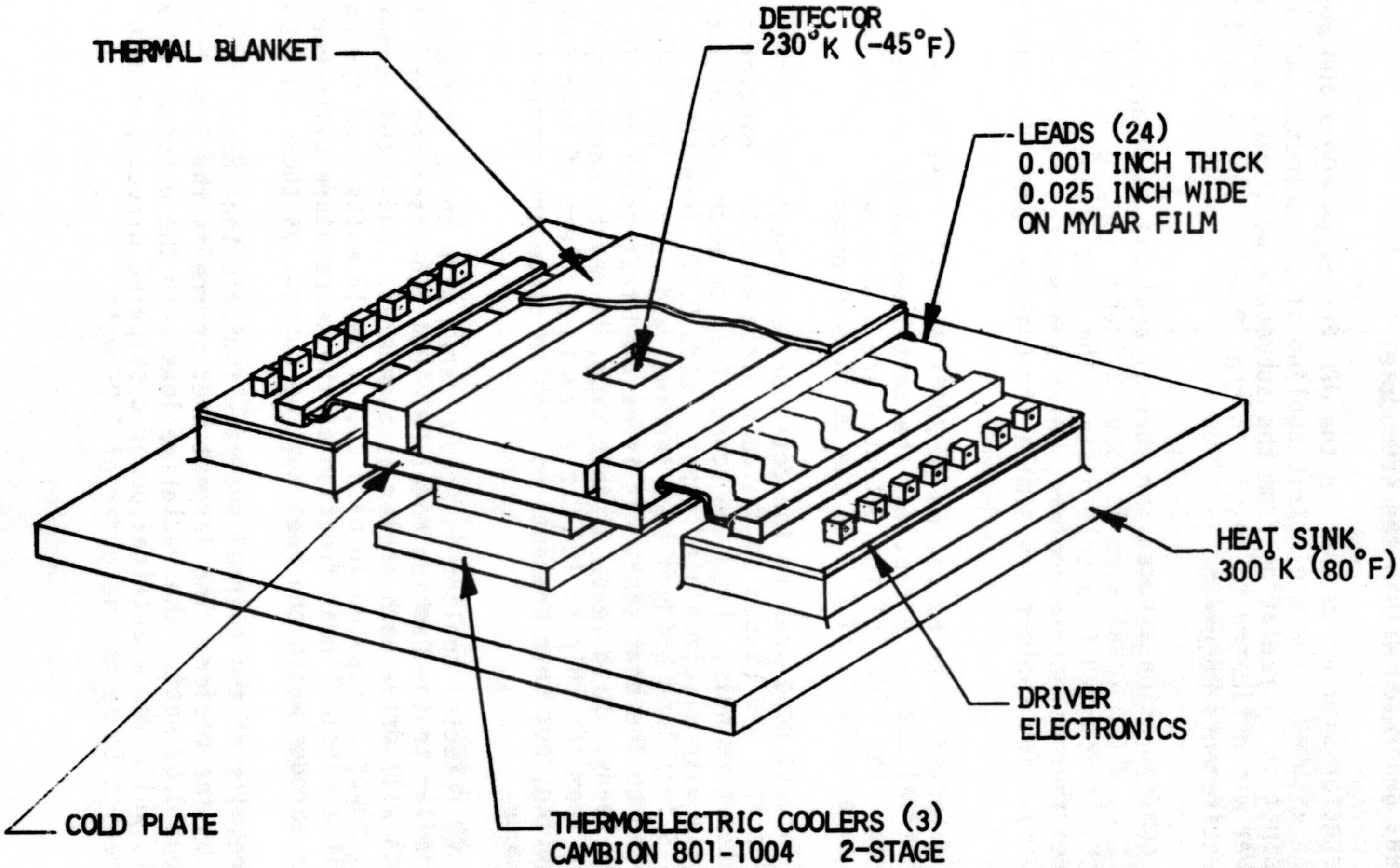

FIGURE 4.2

COOLING CAPACITY OF CCD DETECTOR COOLERS
CAMBION 801-1004 2-STAGE COOLER
WITH HOT TEMPERATURE AT 27°C

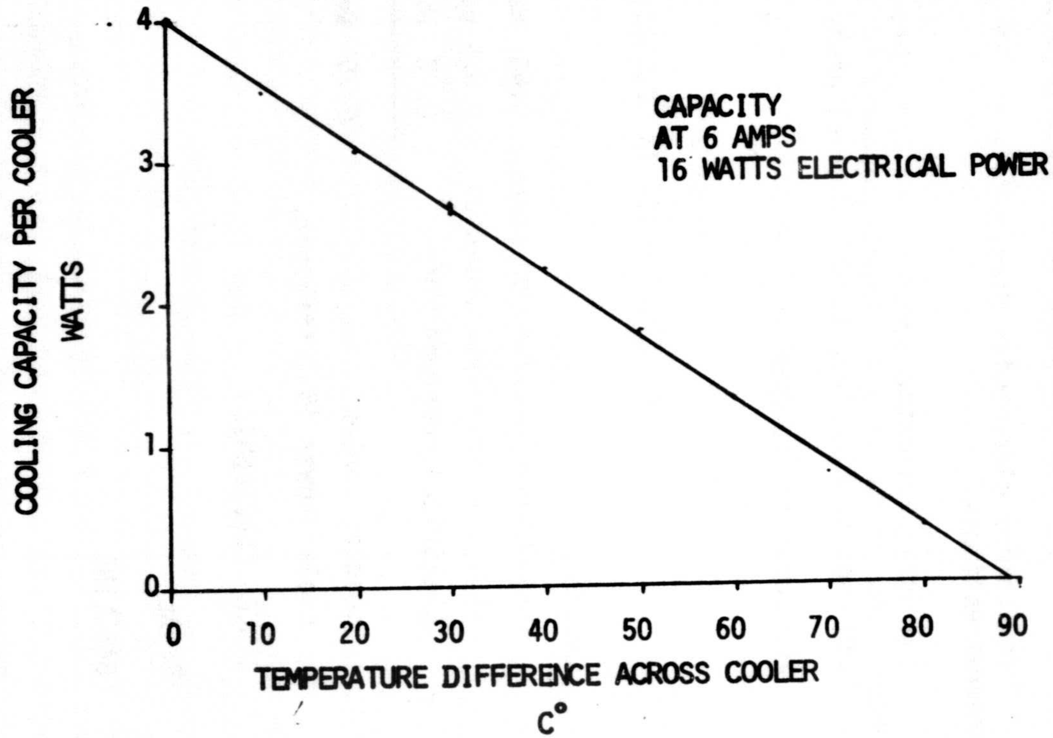

The thermal load on the cooler is about 0.75 watt at a temperature difference of about 70°C. The figure shows that one of the three coolers operating almost continuously would be adequate to maintain the detector temperature. Together, the three coolers will operate with about a 30% duty cycle. The three coolers provide adequate redundance in case of cooler failure. The average power dissipated from the coolers is about 15 watts.

The coolers operate at about 5% efficiency for the required temperature difference; the average power dissipated into the heat sink is about 15 watts.

The camera electronics dissipate about 12 watts, according to the JPL Program estimate.

The total estimated power is, so far, about 27 watts. The baseline power given in the SI Requirements Document is 30 watts. The latter value has been used in Planetary Camera thermal analysis (Section 6).

The power dissipation is summarized in Table 4.1.

TABLE 4.1

POWER DISSIPATION IN CCD DETECTOR

		POWER DISSIPATED
COOLING		
Conductive Loss Through Leads	- 0.63 Watt	
Radiative Loss Into Detector	- 0.075 Watt	
Electrical Power in Chip	- 0.05 Watt	
Load on Cooler	0.75 Watt	
Cooler Power (5% Efficiency)		15 Watts
CAMERA ELECTRONICS		12 Watts
TOTAL		27 Watts
BASELINE		30 Watts

To give the camera submodule adequate radiating area for heat dissipation, a housing considerably larger than that dictated by the 3000 cc volume specified in the SI Requirements Document was assumed. It was assumed that the housing has an emissivity of 0.9, radiating to the outer instrument module wall also with an emissivity of 0.9. It was assumed that there is a 10°F temperature drop from the heat sink at 80°F to the camera submodule wall at an average temperature of 70°F. This is similar to the temperature drops shown by the multi-node thermal model of the SEC orthicon camera submodule.

Under the above assumed conditions, a view factor of 0.67 is required to dissipate 30 watts to the instrument module outer wall at a maximum temperature of 16°F (worst case hot condition from the OTA thermal analysis). This view factor is achieved by use of a thermal reflector to aid in radiation from all sides of the camera submodule housing to the instrument housing.

Figure 4.3 is a thermal diagram of the CCD Camera for the conditions just described.

FIGURE 4.3

CCD CAMERA THERMAL DIAGRAM

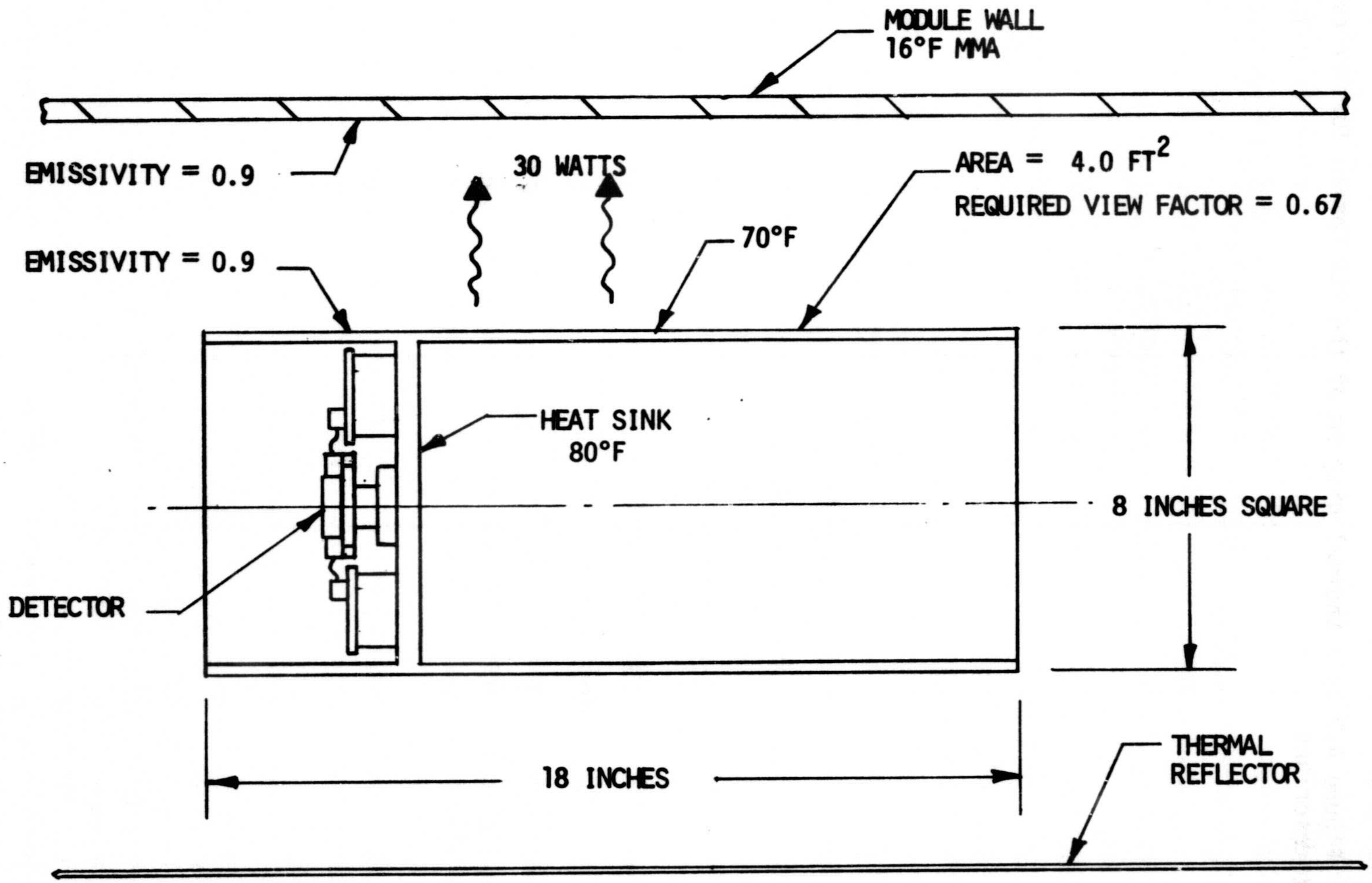

5.0 STRUCTURAL SUBSYSTEM

The structural subsystem consists of an invar optical bench that ties directly to the three support points for the instrument housing. The housing also ties to these three points, and contacts the optical bench at no other point. The optical bench is mounted through thermally-insulating bushings to minimize the heat transfer across the mounting interface. Table 5.1 summarizes the features of the structural subsystem.

TABLE 5.1

STRUCTURAL SUBSYSTEM

Invar Optical Bench

Support Points Common With Outer Housing

Thermally-Insulating Mount Bushings

Figure 5.1 shows the invar optical bench within the instrument housing. It is attached directly to the instrument support points which interface with the OTA. The module housing is also attached to these three points. Consequently, the housing and the optical bench can behave quite independently of each other.

The optical bench consists of a forward bulkhead and a detector bulkhead, connected by suitable framework and bracing to form a rigid structure. The framework extends aft to the aft mounting lug. Between the forward bulkhead and the detector bulkhead is the optics bay with optics and auxiliary devices attached to the two bulkheads or the intervening structure. The optics bay and surrounding structure are enclosed by an aluminum thermal shroud mounted on insulating spacers in such a way that relative thermal expansion between the shroud and the optical bench is permitted. Thermostats and heaters on the shroud control the temperature of the optical bench.

Behind the detector bulkhead is the detector bay. The detector itself is attached to the detector bulkhead. The detector bay has within it, a thermal reflector to direct heat radiated from the detector to the outer wall of the instrument module.

The optical bench is controlled to have a temperature of 70°F, but at its forward attachment points, it is conductively connected to the focal plane structure set at 70°F. To minimize the thermal coupling between these two structures, it is necessary to introduce insulating spacers which are structurally capable of carrying the load of the instrument and maintaining its alignment with respect to the focal plane. For the thermal analysis, a set of insulating spacers as shown in Figure 5.2 was assumed. These spacers would be made of non-metallic material with a conductivity of about 0.2 BTU/HR. FT. °F. With the dimensions shown, the overall conductance through the pair would be 0.106 BTU/Hr. °F. The spacer pair is configured in a symmetrical arrangement so that differential expansion between the spacer itself and the structure to which it is attached will not cause misalignment of the instrument with a resulting image motion or defocus. For the two mounting points, the overall conductance is 0.212 BTU/HR °f, or 0.079 watt/°F.

FIGURE 5.1

INVAR OPTICAL BENCH FOR PLANETARY CAMERA

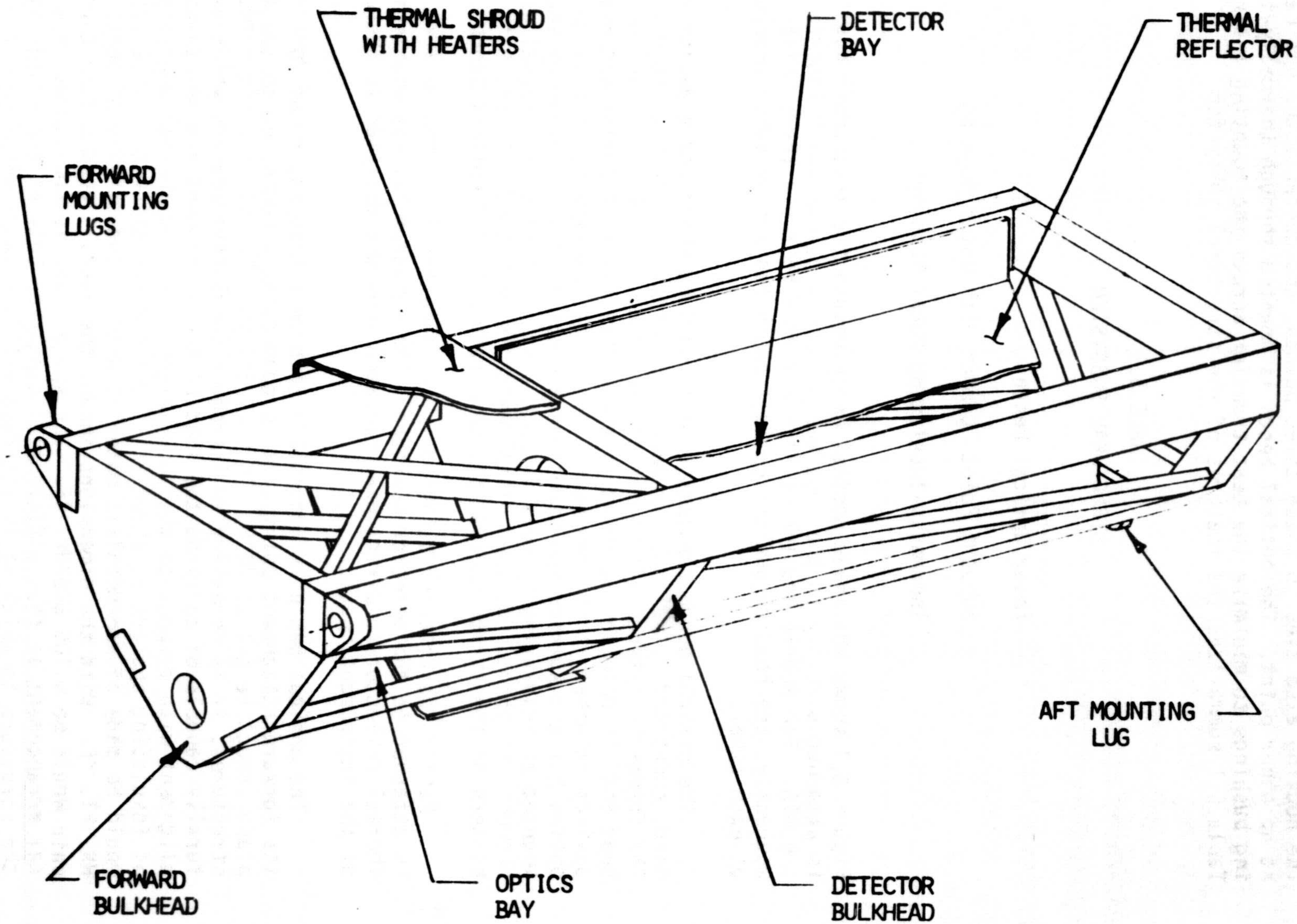

FIGURE 5.2

OPTICAL BENCH SUPPORT INSULATORS

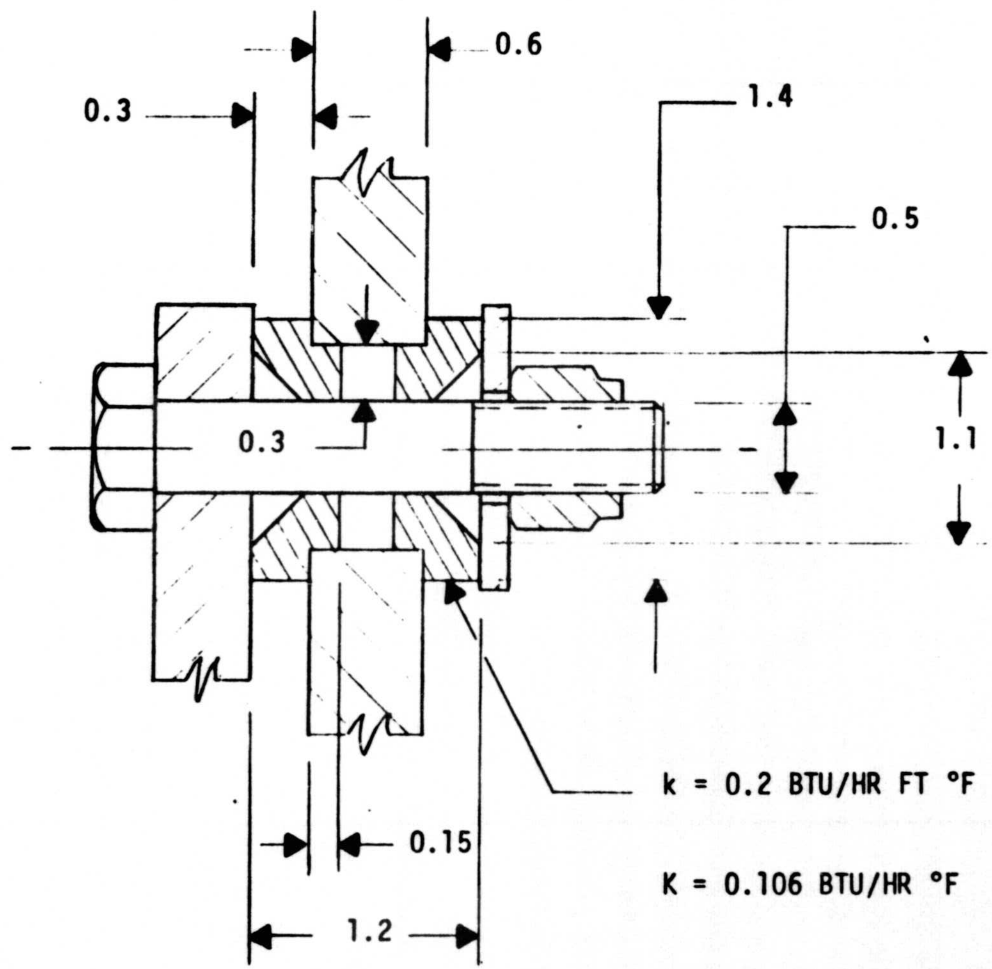

DIMENSIONS IN INCHES

PRECEDING PAGE BLANK NOT FILMED

6.0 THERMAL CONTROL SUBSYSTEM

This section shows the design of the thermal control subsystem and the results of the supporting analysis. The requirements of the thermal control subsystem are to dissipate the heat generated within the instrument and, at the same time, maintain the line-of-sight through the instrument optics stable within the observation time.

A thermal shroud surrounds the optical bench. The shroud contains heaters and thermostats to maintain the optical bench temperature constant. An average of 5 watts thermal power is consumed under coldest conditions. The detector radiates the heat it generates to the outer wall of the instrument module, directly from one side and via a thermal reflector from the other side. The line-of-sight through the relay optics is maintained stable to within 0.003 arcsecond in over a period of one hour. Table 6.1 summarizes the features of the thermal control subsystem.

TABLE 6.1

THERMAL CONTROL SUBSYSTEM

Thermal Shroud and Thermostatic Control for Optical Bench
Heat Dissipation by Radiation to Outer Instrument Module Wall
5 Watts Average Thermal Control Power
Thermal Reflector to Maximize View Factor for Detector
0.0005 Arcsecond Thermally-Induced Image Motion in Five Minutes

6.1 Thermal Diagram of Planetary Camera

Figure 6.1 is a thermal diagram of the Planetary Camera as it was analyzed. The CCD Camera submodule dissipates 30 watts. The radiating area of the sides of the camera submodule body is 4 ft.^{2}. It was assumed that the effect of the thermal reflector in the detector bay would be to create a 67% view factor between the camera submodule and the outside wall of the instrument module. A 90% emissivity (flat black) was assumed for the camera submodule surface and the instrument module wall. The result of this is that the average camera submodule temperature is about 70°F, depending upon the internal power dissipation when radiating to a wall of 16°F, which represents the maximum wall temperature derived from the OTA thermal model with 400 watts of SI dissipation, including 100 watts in each instrument module.

A thermal shroud surrounding the optics bay of the optical bench maintains that area at 70°F via thermostats and heaters in two zones on the shroud. The outside of the shroud has a low emissivity of 2%, while the inside of the shroud and the surfaces of the optical bench structure within the shroud are black for maximum radiative transfer within the shroud. By this means, it is estimated that the temperature level of the optical bench structure within the shroud will be maintained within $\pm$ 1°F. The optical bench is insulated from the focal plane structure by insulating spacers at the two attachment points. At each point, the thermal conductivity is 0.106 BTU/Hr.°F. This is equivalent to 0.08 watt/°F for both of them. The camera submodule is similarly insulated from the optical bench at four mounting points. A conductivity of 0.006 watt/°F is assumed for each, for a total of 0.024 watt/°F.

FIGURE 6.1

THERMAL DIAGRAM OF PLANETARY CAMERA

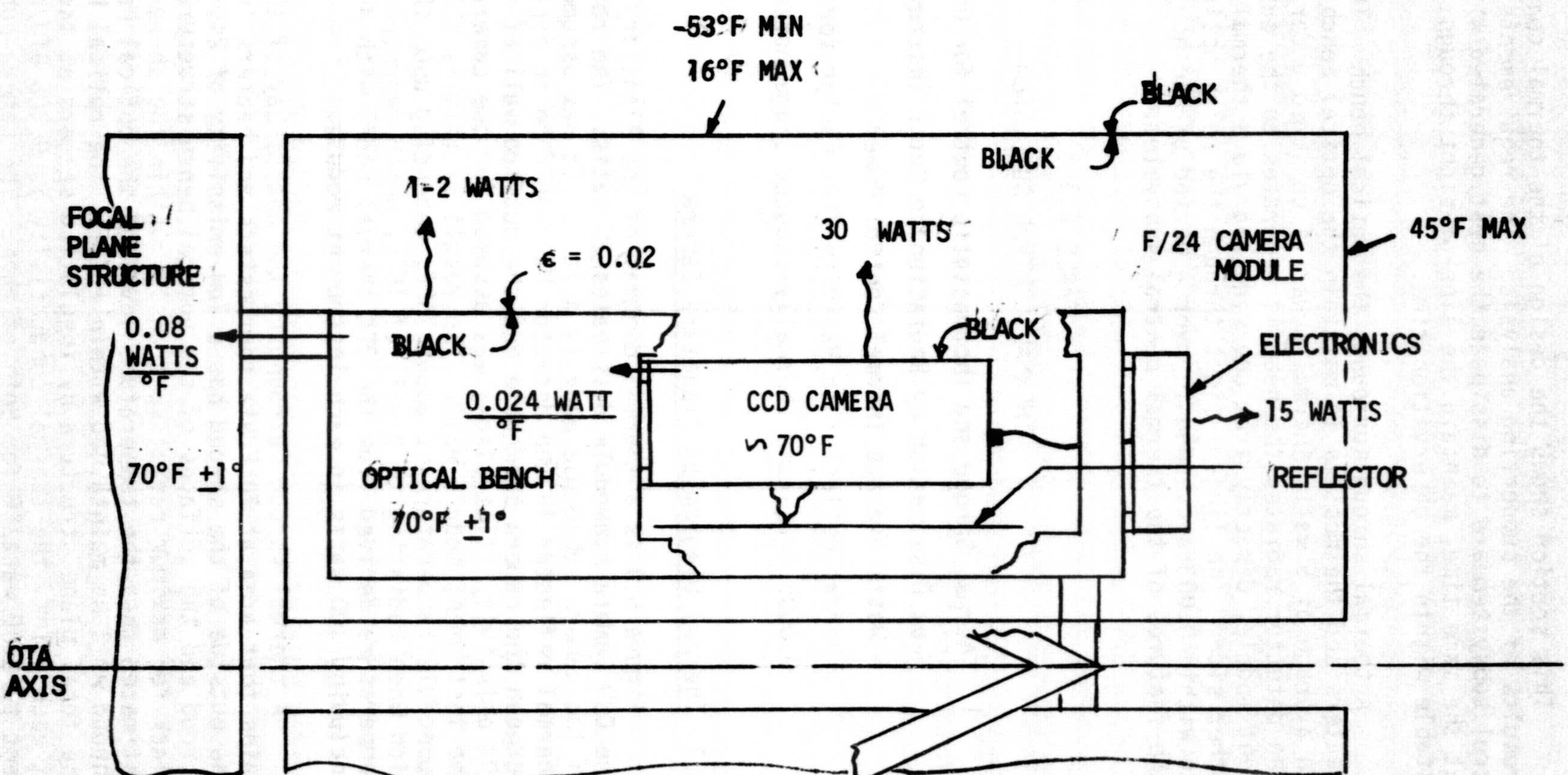

Power at 1-2 watts will be radiatively dissipated from the outside wall of the thermal shroud, depending upon whether the outside wall of the instrument module is at its maximum temperature of 16°F or its minimum temperature (all SIs shut off) of -29°F. This is based upon a radiating area of 5.2 ft^2 with on 80% view factor and an emissivity of 2%.

The electronics box radiates to the aft wall of the module, which has a maximum temperature of 45°F. The forward and inner walls of the instrument module have low-emissivity surfaces to make them, in effect, adiabatic.

6.2 Image Motion From Thermal Distortions

Relative displacements between the optical elements and the detector in the camera, and displacements of the camera as a whole relative to the OTA focal plane, can result in image motions if the displacements occur during the course of an exposure. Figure 6.2 shows how the optical element displacements relate to image motion.

In this diagram, Δy_{ii} is the displacement of the input image, Δy_p and $\Delta\theta_p$ are the displacement and tip of the first mirror of the relay, Δy_s and $\Delta\theta_s$ are the displacement and tip of the second mirror, Δy_{io} is the displacement of the output image and Δy_d is the displacement of the detector surface. The relationship given at the top of Figure 6.2 is derived from first-order optics and expresses the relative motion between the output image and the detector surface as a function of the motions of the input image and the elements in the optical train.

6.3 Sensitivity of Optical Bench to Thermal Gradients

A very rough analysis was made to estimate the sensitivity of the optical bench to thermal gradients in terms of image motion-producing distortions. It is the relative motions of the forward bulkhead and the detector bulkhead which would produce relative motions between the optical elements. Simple geometric analysis of the trusswork connecting the two bulkheads gave a rough estimate of what relative motions would result from temperature differences between the members of the trusswork. First, displacement sensitivity was estimated by assuming that the diagonal member was elongated by a 1°F temperature increase, using a thermal coefficient of expansion for invar of 0.7×10^{-6}/°F. The resultant sensitivity was 1.7 micrometer decenter/°F. Similarly, an assumed temperature change of one of the parallel elements of the truss gave a tip sensitivity of 2.6 microradians/°F. Figure 6.3 shows the deflection sensitivities to thermal gradients in the truss.

These sensitivities were coupled with the optical system sensitivities to estimate the image motion that could be expected to result from changes in the thermal gradients within the invar optical bench.

6.4 Image Motion From Changes in Heat Flow

The heat flow into and out of the optical bench varies with time, causing temperature gradients within it to vary with time. Variations during an exposure will cause image motions at the detector because of the resulting distortions of the optics bay and movement of the optical elements.

FIGURE 6.2

IMAGE MOTIONS FROM THERMAL DISTORTIONS OF F/96 PLANETARY CAMERA

$$\Delta y_{io} - \Delta y_d = -4\,\Delta y_{ii} - 6.72\,\Delta y_\rho - 4m\,\Delta\theta_\rho + 3.72\,\Delta y_s + 1.3m\,\Delta\theta_s - \Delta y_d$$

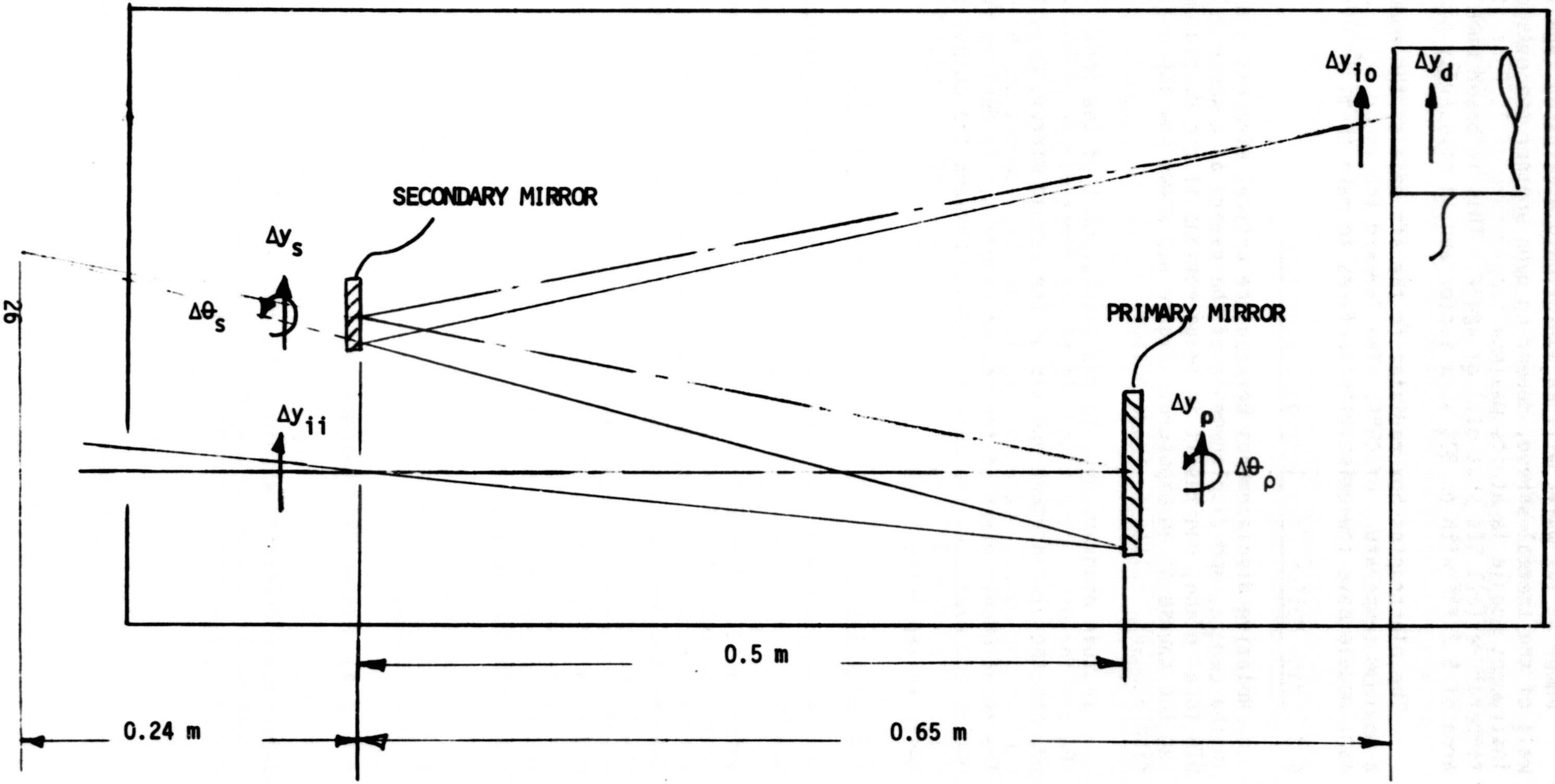

FIGURE 6.3

SENSITIVITY OF OPTICAL BENCH TO THERMAL GRADIENTS

RELATIVE DECENTER OF FORWARD AND AFT BULKHEADS

$\alpha = 0.7 \times 10^{-6}/°F$

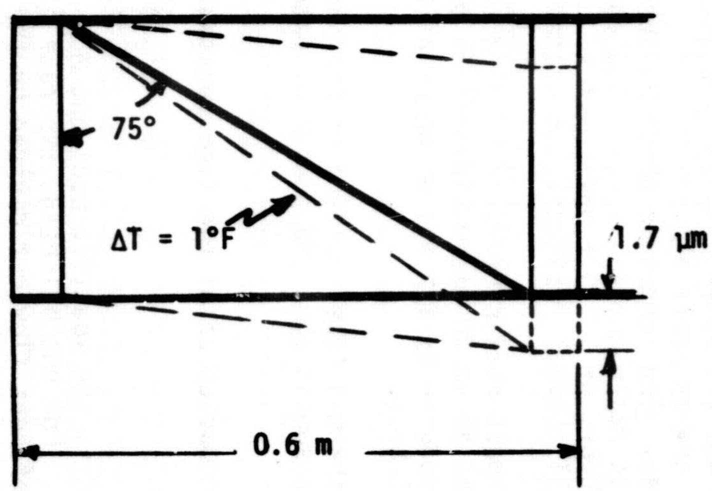

RELATIVE TIP OF FORWARD AND AFT BULKHEADS

$\alpha = 0.7 \times 10^{-6}/°F$

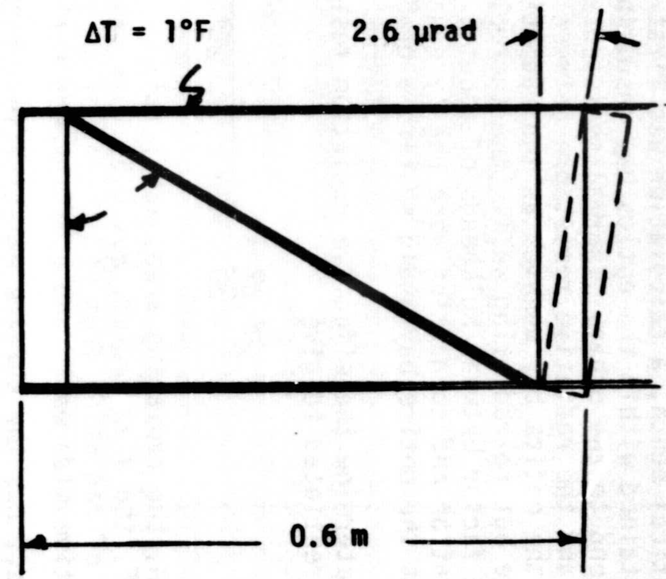

To estimate what motions could be expected from changes in heat inputs to the optical bench, a calculation was first made of the temperature gradient sustained within the optics bay resulting from steady-state heat flow from one end to the other. Thermal resistance along the trusswork was calculated, and the radiative resistance between the bulkheads was calculated, assuming the optics bay behaves as two radiating plates enclosed by nonconductive but re-radiating walls (the thermal shroud). This gave an effective view factor between bulkheads of about 0.5. The thermal resistances from radiation and conduction were nearly equal in magnitude, and it was found that the optics bay would sustain a gradient of about 4.0°F/watt.

To determine the effective radiation resistance, the radiation equation was differentiated to give

$$\frac{\Delta T}{\Delta Q} = \frac{1}{4FA\ \varepsilon_1\ \varepsilon_2\ \sigma T^3}$$

in which A, the radiating area, was 1 ft^2,

F, the view factor, was 0.5, this case being similar to the textbook case of radiation from end-to-end of an enclosure with re-radiating, nonconductive side walls and a 1:1 aspect ratio.

ε_1, ε_2, the surface emissivities, both 0.9

σ, the Stephan-Boltzman constant, equal to 0.17×10^{-8} BTU/hr. sq.ft.R^4

T, the average temperature, 70°F, or 530°R.

The radiation resistance was computed to be 2.44°F/BTU/hr., or 6.57°F/watt.

In computing the conduction resistance for the trusswork of the optical bench, it was estimated that the trusswork has a total peripheral distance of 54 inches and an average thickness of 0.05 inch, giving a 2.7 in^2 cross sectional area. The length is about 20 inches. A conductivity of 30 BTU/hr ft°F was used to represent the invar. The conductive resistance computed was 2.96°F/BTU/hr, or 10.11°F/watt. These two resistances were combined to give the overall thermal resistance as stated above.

The image motion produced by gradients within the optics bay was calculated to be about 20 micrometers/°F by using the root sum square value of the motions produced by tip and decenter of the first relay element at the detector bulkhead.

The thermal time constant of the optics bay was calculated to be about 4 hours, assuming about 30 pounds of material in the two bulkheads, a specific heat of 0.1 BTU/lbm °F, and the thermal resistances already calculated.

The computation of the time constant was based upon the relationship

$$T = \frac{\Delta T\ \ CM}{4\Delta Q}$$

in which C is the specific heat and M is the mass of the material in the bulkheads. For one bulkhead, the rate of temperature drop is proportional to the rate of heat flow out divided by the product C x M for that end alone. At the other end, the temperature will be rising at an equal rate, doubling the rate of the differential temperature change. The total mass of the bulkheads is twice that of one, and these two factors of two explain the factor of four in the relationship given above.

The image motion within a one-hour time period produced by a given change in the heat input was calculated by dividing the steady-state gradient by the time constant and multiplying by the optical sensitivity. The resulting estimated sensitivity to changes in the heat input was 20 micrometers/watt.

Table 6.2 summarizes the factors which determine the overall sensitivity in terms of image motion from a change in heat flow.

TABLE 6.2

IMAGE MOTION IN F/96 PLANETARY CAMERA
FROM CHANGES IN HEAT FLOW

Steady-State Gradient in Optical Bench From Heat Flow Thru Optics Bay	4.0°F/Watt
Image Motion Produced by Gradient	20μm/°F
Thermal Time Constant of Optics Bay	4 hours
Image Motion in One Hour	20μm/Watt

6.5 Thermally Induced Image Motion

The Scientific Instrument Requirements Document gives five minutes as the maximum exposure time for the camera, and so image motions within this time period have been calculated as well as the motion expected within one hour. The motions expected from various sources are tabulated in Table 6.3.

First, it was assumed that the average temperature of the optical bench changes by 1°F, maximum. If the thermal shroud changed suddenly by this amount, the optical bench would change by only 2% of that amount within five minutes because of its four hour time constant. The resulting motion arises from the growth of the structure and the relative motion between the optics and the OTA focal plane. In the worst case, a temperature gradient of 0.02°F would arise in 5 minutes, or 0.24°F in 1 hour.

A change in the focal plane structure of 1°F changes the heat conducted out of the optical bench through the insulating supports. The result is a change in the gradients within the optical bench.

A change in the detector temperature also causes a change in the heat flow through the optical bench, in this case, through the insulating spacers between the camera submodule and the optical bench. The camera submodule temperature will be changing continuously, since it will probably not be fully warmed up when the exposure starts, and since its temperature will be affected by changes in the temperature of the instrument module wall. It was assumed that the camera submodule might change its temperature by 1°F in five minutes, although this is rather extreme. The OTA thermal analysis shows that the instrument module outer wall will change temperature by only about 2°F in an hour as the result of other SIs being turned on.

Each filter motor draws an average power of about 2.6 watts while turned on. The maximum energy input from all four wheels is only 0.01 watt-hour, however. It was assumed that 3/4 of this energy would be radiated away from the optical bench.

The temperature gradient in this case was calculated from the energy input and the thermal mass of the detector bulkhead.

The temperature controllers on the thermal shroud will maintain its temperature within ± 1°F in a limit-cycling fashion. The limit cycling will be much faster than the time constant of the optical bench, however, and so the resulting changes in the gradients in the optical bench will be greatly attenuated. A factor of ten attenuation was assumed for motion in one hour, or 120 times attenuation for motions within five minutes. The thermal shroud blocks the effects of variations of the temperature of the instrument module walls.

The root-sum-square total motion after five minutes was calculated to be 0.61 micrometer (0.0005 arcsecond in object space). Adding in the OTA motion gives a total RMS motion of about 0.007 arcsecond. After one hour, the motion within the camera is 7.3 micrometers (0.0065 arcsecond), with a total motion, including the OTA motion, of 0.010 arcsecond.

TABLE 6. 3

THERMALLY INDUCED IMAGE MOTION

	MICROMETERS MOTION AT F/96	
	FIVE MINUTES	ONE HOUR
Average Temperature Change - ± 1°F	0.4	4.8
Change in Focal Plane Structure - ± 1°F	0.13	1.6
Change in Detector Temperature - 10°F	0.4	4.8
Filter Operation -	0.04	0.04
Thermal Control Limit Cycling - ± 1°F	0.17	2
RSS Total	0.61 (0.0005 Arcsec)	7.26 (0.0065 Arcsec)
Including OTA Motion	(0.007 Arcsec)	(0.010 Arcsec)
Required	(0.007 Arcsec)	

7.0 MECHANISMS

The mechanisms in the Planetary Camera which require careful design for reliability and minimum dynamic disturbance are:

Filter Assembly (Four Wheels)

Capping Shutter Assembly

Exposure Control Shutter
(Integral with Camera Shutter)

The filter complement from the HRC FID is shown in Table 7.1. There are 28 elements in all, seven on each of four wheels. The eighth position on each wheel is open.

TABLE 7.1

F/48, F/96 PLANETARY CAMERA
FILTER COMPLEMENT

2200	8000
2800	8500
U	9000
B	9500
V	10000
R	10500
I	11000
4000	POLARIZER 1
5000	POLARIZER 2
5500	POLARIZER 3
6000	87-C
6500	GLASS
7000	ND-1
7500	ND-2

The four filter wheels are stacked up immediately in front of the camera submodule. Each wheel has eight positions.

Each filter wheel is indexed by a stepper motor, similar to Clifton Industries Model MSA 15-AS-1 permanent magnet two-phase stepper with 90° rotation per step. Each wheel has a rotary inertia of about 3.3 lbm in^2, or 9,600 GM CM^2. The stepper can drive this load through a 50:1 reduction at a rate of 50 pulses/second. Twenty-five steps are required to move one filter position.

The stepper motor has a winding resistance of 150 ohms. At 28 volts, assuming a 50% duty cycle for the pulses, the motor dissipates an average 2.6 watts. Details of the electrical system are described in Section 10.

Figure 7.1 is a schematic of the drive system for each wheel.

The capping shutter allows light to enter the aperture of either of the relays, the standard star calibration system, or none of them, and hence has four positions. The shutter consists of a counter-balanced blade driven through a 30:1 gear reduction by a stepper motor like that used for the filter wheels. The rotary inertia of the blade with its counter-balance is about 1.1 lbs $in.^2$, or 3100 GM CM^2 based upon 0.06 inch thick aluminum. The stepper motor can drive this inertial load through the gear train at 50 steps/second. Four steps are required to drive the shutter from one extreme to the other, requiring 0.08 seconds. A shutter position is controlled with feedback from a position sensor. A diagram of the shutter and its drive is shown in Figure 7.2.

The exposure control shutter is assumed to be a part of the camera submodule in order that it can be as close as possible to the focal plane. This shutter would have two blades which move across the focal plane at constant velocity. The exposure time is determined by the slit width between the blades. Since this mechanism operates simultaneously with an exposure, good dynamic design is required.

FIGURE 7.1

FILTER WHEEL
FOR F/24 FIELD CAMERA

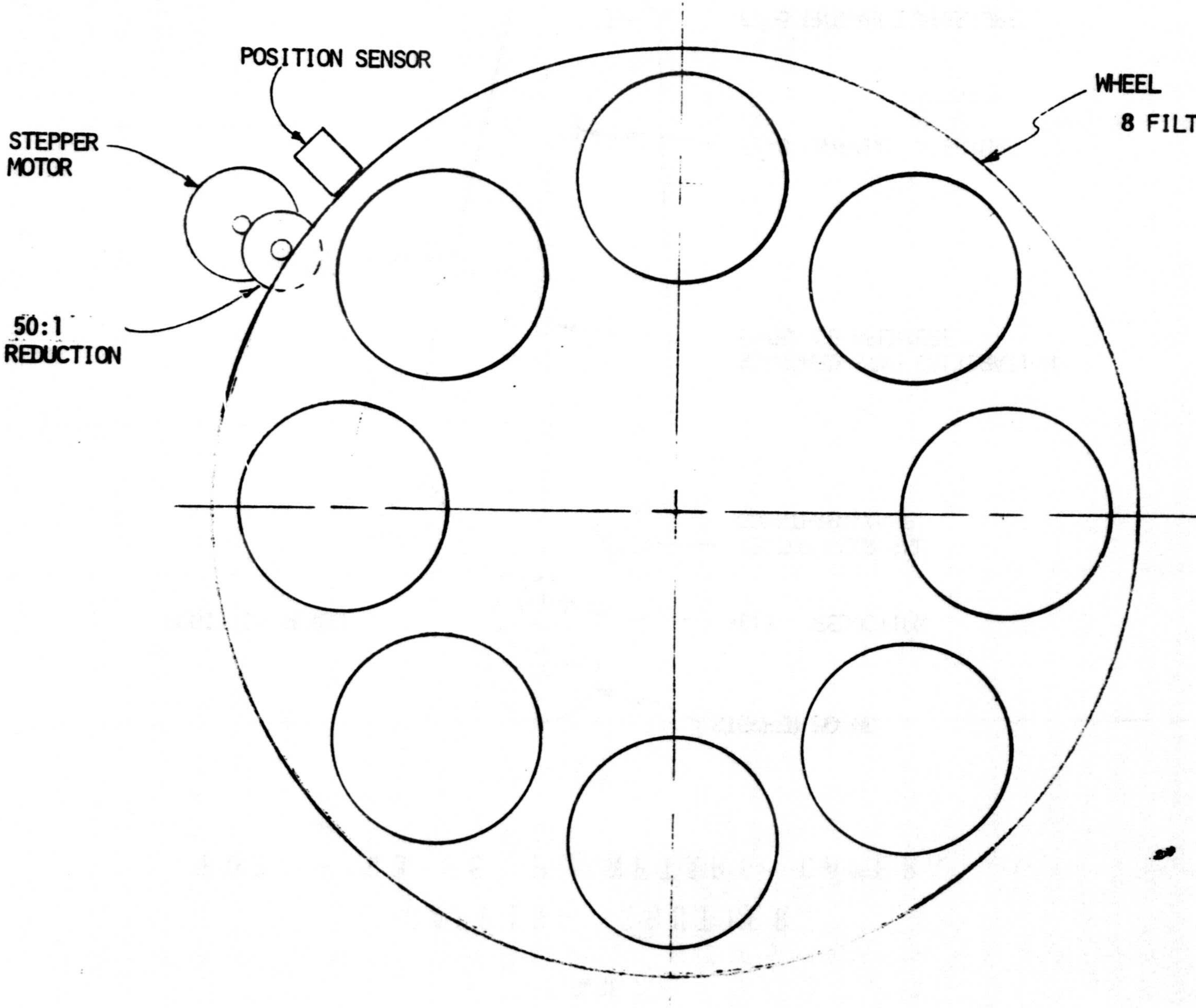

FIGURE 7.2

CAPPING SHUTTER
FOR F/48, 96 PLANETARY CAMERA

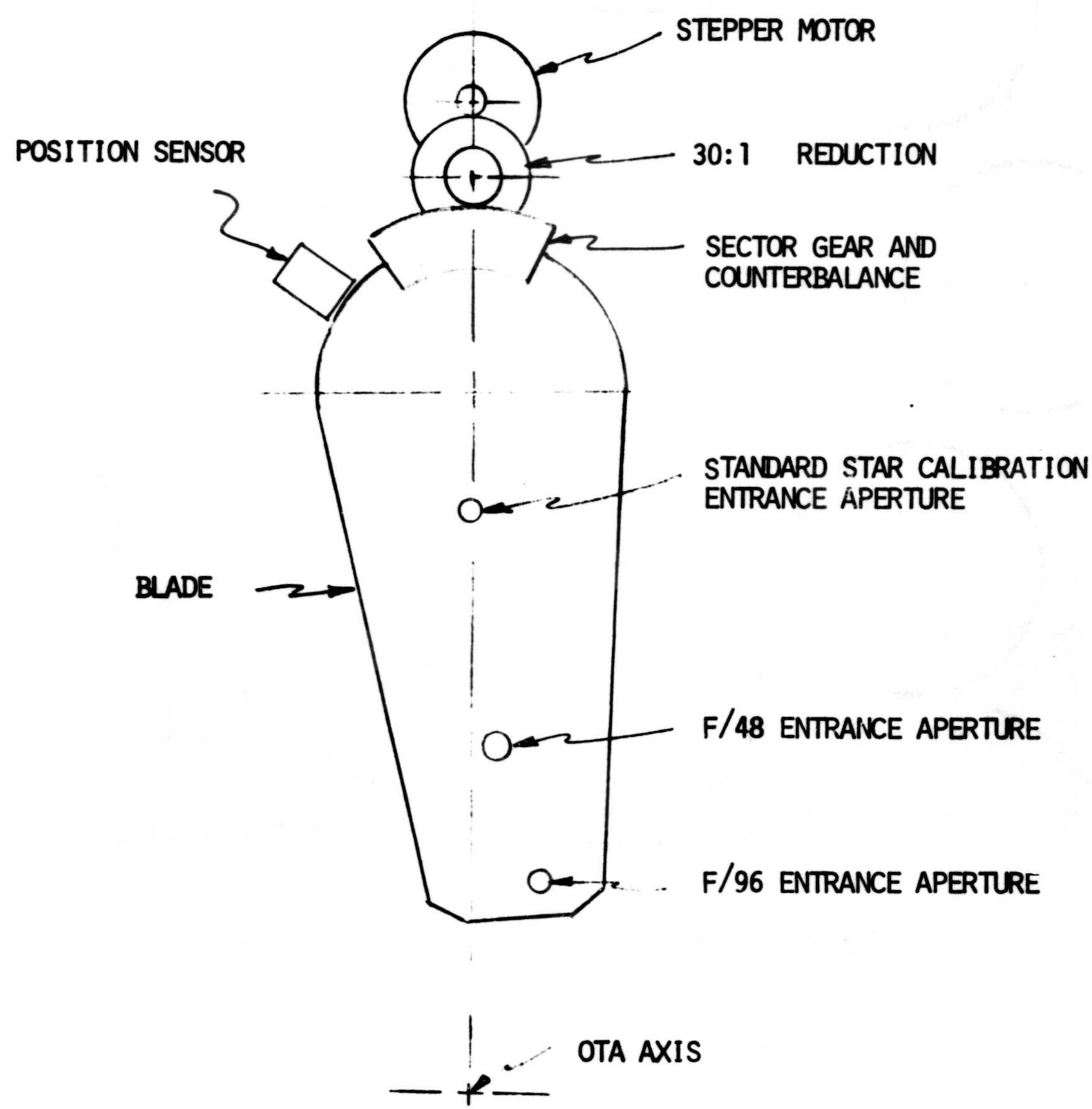

8.0 DYNAMIC DISTURBANCES

Figure 8.1 shows the dynamic disturbances to the LST from operation of the mechanisms within the F/48, F/96 Planetary Camera.

Included are profiles for the operation of one filter wheel and the capping shutter.

The disturbance to the body pointing resulting from operation of the camera mechanisms was estimated from the characteristic step motions of the mechanisms, the inertias of the mechanisms, an assumed inertia of 121×10^6 lbm in^2 for the spacecraft, and an assumed body pointing control system gain crossover frequency of 3 radians per second. For disturbances longer than 0.33 second, the reciprocal of the gain crossover frequency, the effects were computed as the step change in velocity of the component divided by the gain crossover frequency, multiplied by the ratio of the component inertia and the body inertia. For the F/48, F/96 capping shutter, which operates in a time shorter than 0.33 second, the body motion was calculated as the step positional change of the shutter times the ratio of the inertias.

The assumption of 3 radian/second for the gain crossover frequency was conservative. Normally the filters would not be operated during an exposure. Smaller disturbances would result if the filters were driven at a lower rate.

The results of the calculations are shown in Table 8.1. Only the filter wheel appears to cause a marginally significant disturbance. At most, two filter wheels would operate at a given time: one returning to its open position, the other advancing to the required filter position.

The vibrational disturbance of operating the camera mechanisms was estimated by assuming that the stepping frequency was in resonance with the closest vibrational mode of the OTA as determined from the OTA structural analysis. Assuming the resonant build-up was limited by damping which was 0.5% of critical, the line-of-sight vibrational motions as shown in this figure were calculated. Vibrations at this frequency would damp out very quickly after the disturbance stopped, even with the low damping assumed. The vibration would damp out to 20% of the maximum amplitude after one second, and 4% after two seconds of settling time.

Table 8.2 shows the peak disturbances computed. It is highly unlikely that the resonance conditions described above would actually be attained.

TABLE 8.1

BODY POINTING ERRORS FOLLOWING OPERATION
OF CAMERA MECHANISMS

COMPONENT	CHARACTERISTIC STEP MOTION	EFFECT ON BODY POINTING 3 RAD/SEC GAIN CROSSOVER FREQ.
F/48, 96 FILTER	1.57 RAD/SEC	0.003 ARCSEC
F/48, 96 SHUTTER	0.052 RAD	0.0001 ARCSEC

TABLE 8.2

VIBRATIONAL DISTURBANCES FROM
OPERATING CAMERA MECHANISMS

COMPONENT	WORST-CASE RESONANT BUILD-UP WITH 0.5% DAMPING AT 51.8 HZ MODE
F/48, 96 Filter	0.001 Arcsec
F/48, 96 Shutter	0.003 Arcsec

FIGURE 8.1

DYNAMIC DISTURBANCES FROM F/48, 96 PLANETARY CAMERA

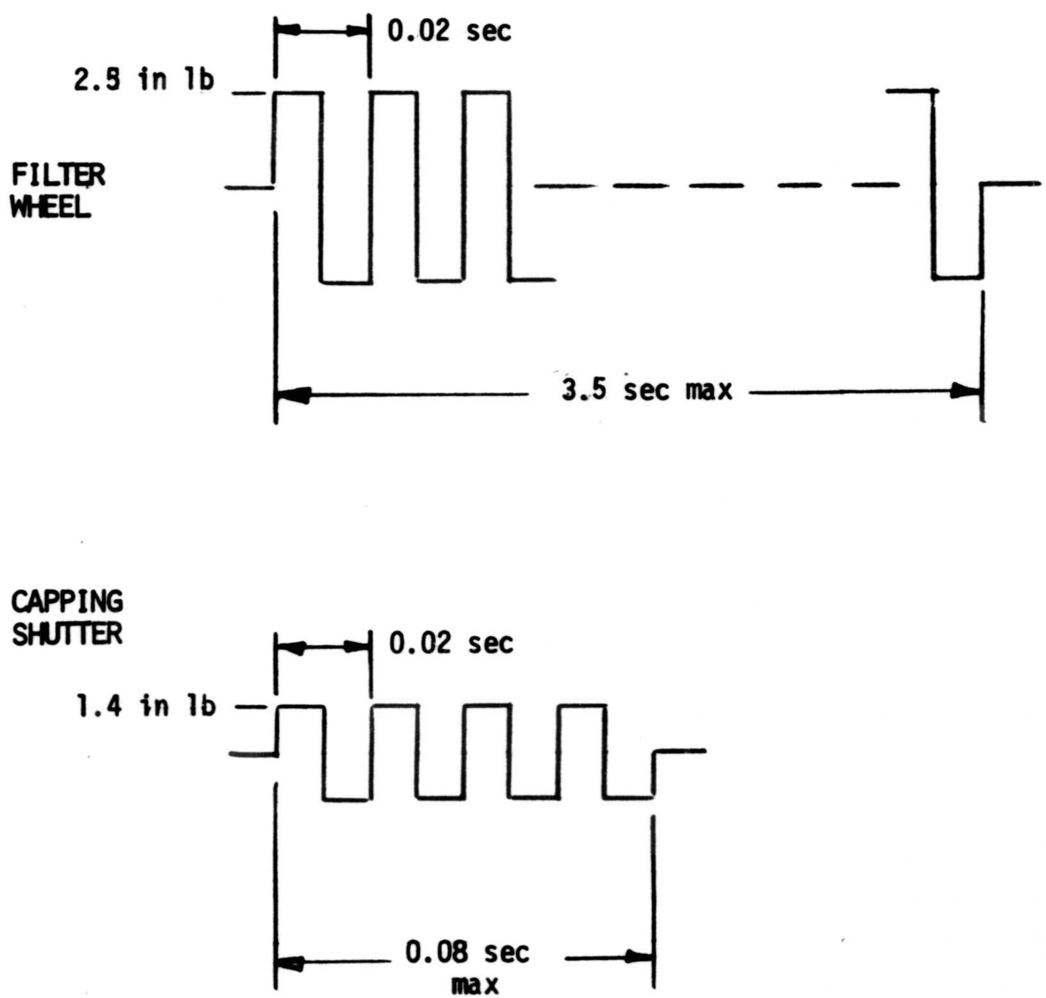

9.0 WEIGHT

Table 9.1 gives the estimated weight for the Planetary Camera. The center of gravity for the camera lies approximately 30 inches behind the OTA focal plane.

TABLE 9.1

PLANETARY CAMERA ESTIMATED WEIGHT

	Weight
Camera Submodule	37 lb.
Optical Bench	60
Filter Assembly	6
Capping Shutter Assembly	2
Relay Optics and Fittings	6
Calibration Optics and Fittings	2
Thermal Shroud	9
Thermal Reflector	6
Electronics Box	10
Connector Assembly	3
Module Housing	47
Handles, Registration Fittings	10
Fasteners, Cabling, Paint, etc.	20
Total	218 lb.

10.0 ELECTRICAL SUBSYSTEM

The electrical subsystem design has been carried to the functional block diagram level. Figure 10.1 shows the functional diagram of the Planetary Camera. The Planetary Camera consists of four functional assemblies:

1. DETECTOR ASSEMBLY - The detector assembly consists of the five blocks shown in Figure 10.1

    1. 400 x 400 Pixel CCD
    2. Detector Thermal Control
    3. Video Electronics
    4. CCD Power Regulator

    The preliminary design of the thermal cooling system consists of the detector chip mounted on a cold plate which, in turn, is connected to a heat-sink bulkhead within the detector module via three two-stage thermoelectric coolers. The cold plate is thermostatically maintained at 230°K (-45°F) by the coolers pumping to the heat sink at about 300°K (80°F). The average cooling power is about 15 watts. One of the three coolers continuously drawing six amperes would be capable of maintaining the cold plate temperature.

    Previous investigations of possible types of shutters for use in spaceborne electro-optical cameras have suggested that the focal plane type of shutter, consisting of a curtain with a rectangular aperture slit which is driven across the image format at constant velocity will meet requirements of high shutter efficiency and minimal mechanical complexity.

2. DUAL APERTURE SHUTTER ASSEMBLY - Each shutter is a four position unit driven by a stepper motor/sector gear mechanism. The four positions are:

    1. All Blocked
    2. Imaging Aperture Open (F/96)
    3. Imaging Aperture Open (F/48)
    4. Calibration Aperture Open

    The shutter assembly will employ position feedback to verify shutter position. The feedback unit will consist of a suitably filtered source and indium antimonide photo diodes.

3. CALIBRATION ASSEMBLY - The calibration assembly provides two current levels to a calibration lamp. The current levels provide for calibrated irradiance levels at the detector. A pair of silicon detectors are employed to monitor the output of the calibration source.

4. FILTER MECHANISM ASSEMBLY - The filter mechanism for the Planetary Camera consists of four coaxial, eight position wheels. One position in each wheel will be open.

Each wheel will be driven by a stepper motor/gear train. Twenty-five steps will be required between filter positions. The motor will operate at 50 steps/second. The maximum time to index from one position to any other will be 3.5 seconds (assuming unidirection rotation).

Each wheel will employ position feedback to verify filter position. The outer edge of each wheel will contain a zero reference reflective strip. A source/detector pair will be used with each wheel to sense the zero reference positions.

The Planetary Camera also contains the following electronics:

1. INSTRUMENT CONTROL UNIT - The instrument control unit provides command decoding and unit sequencing for non-detector specific functions and contains the "INSTRUMENT OFF" status sensors. The unit decodes shutter, filter position, and calibrate commands and then activates the appropriate assemblies. In addition, it also initiates data readout from the CCD assembly.

2. POWER CONDITIONER UNIT - The power conditioner unit consists of two redundant regulators and a power switching unit.

   The power switching unit, designed free of single point failures, responds to a power command from the digital interface unit and provides the capability to select either regulator and to power the selected regulator from either BUS A or BUS B or both.

3. REDUNDANT DIGITAL INTERFACE UNITS (DIUs) - The Planetary Camera interfaces with the SI Communications and Data Handling System via redundant DIUs.

FIGURE 10.1

F/48, F/96 PLANETARY CAMERA
FUNCTIONAL DIAGRAM

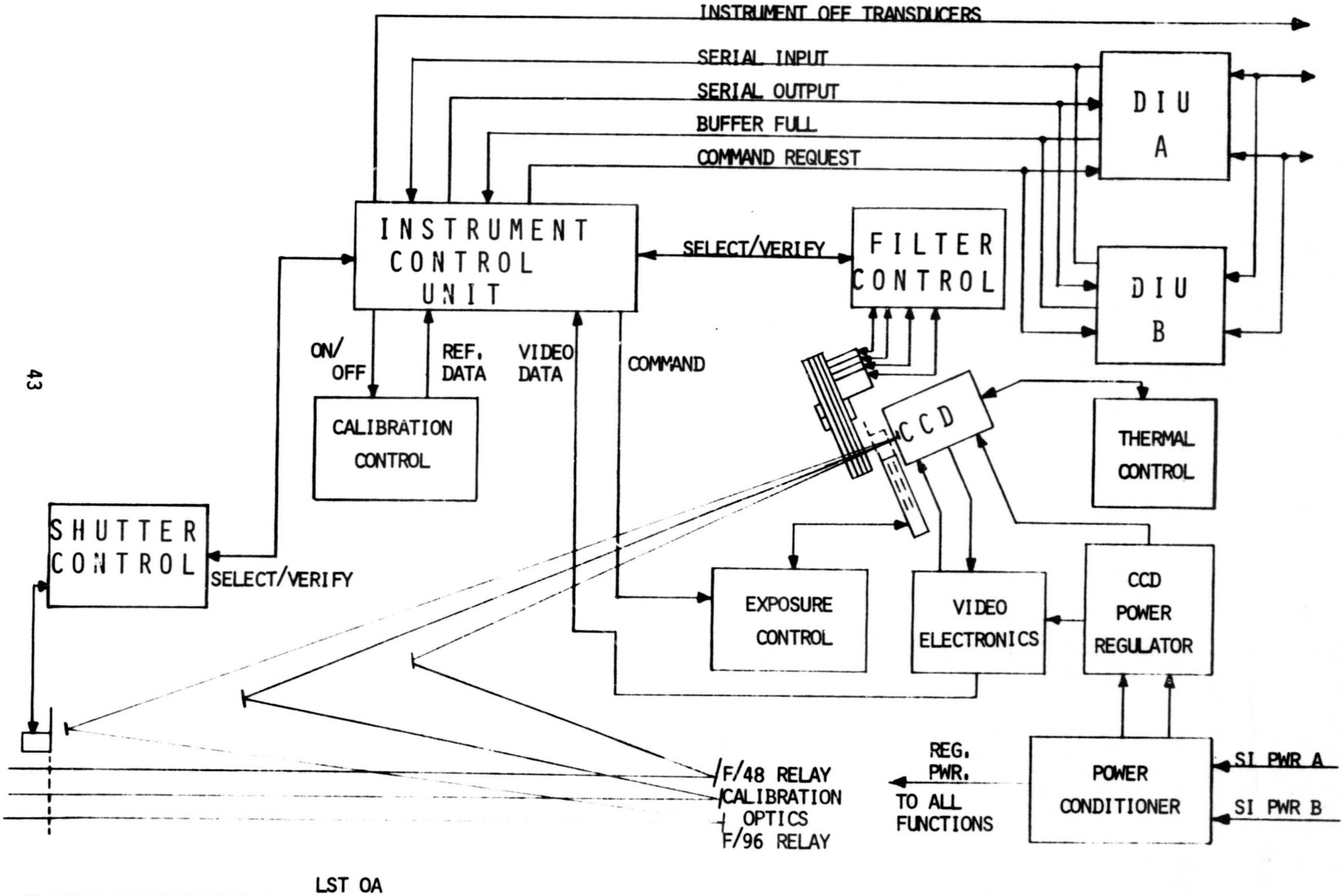

11.0 POWER

Figure 11.1 shows the power profile for the Planetary Camera, including time for warmup, calibration, exposure, and readout. The makeup of the total power is as follows:

Camera Submodule	30 Watts
Two Digital Interface Units	8 Watts
Capping Shutter Control	5 Watts
Exposure Control	5 Watts
Filter Control	5 Watts
Calibration	1 Watt
Thermal Control	5 Watts

The power conditioner unit is assumed to have an efficiency of 75%. Its regulation applies to everything except the thermal control power. The maximum power, including the power consumed in the power conditioner unit is 77 watts.

FIGURE 11.1

F/48, F/96 PLANETARY CAMERA POWER PROFILE

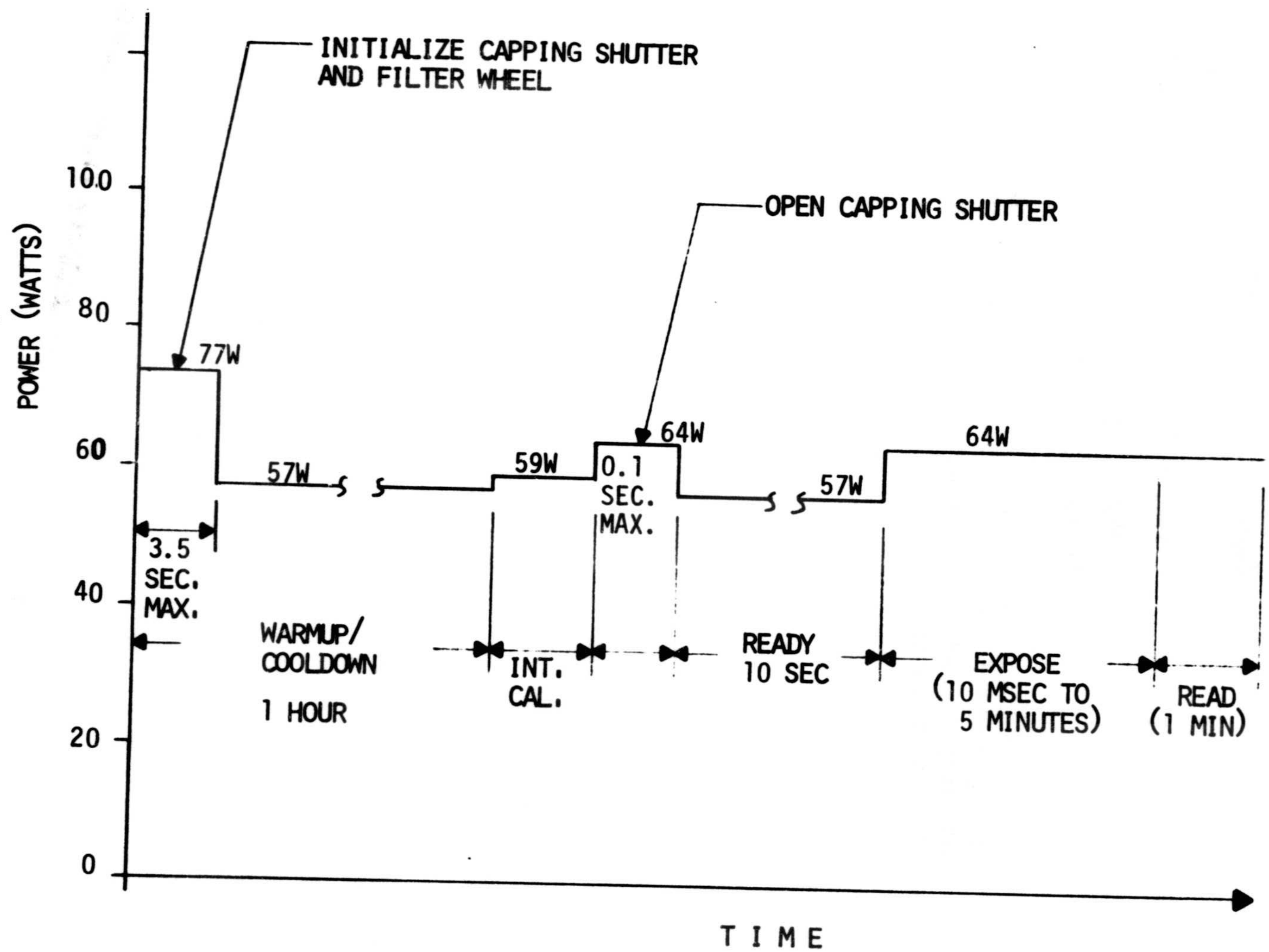

12.0 COMMAND AND DATA LISTS

Table 12.1 gives the command list for the Planetary Camera and the number of bits comprising each command. The commands are input according to the standard command format.

The power select command determines which of the two redundant power regulators and power busses are used.

The mode select command sets the camera in one of the following modes:

Activate Standby

Activate Expose Sequence

Activate Read Sequence

Activate Calibration Sequence

The calibration command determines which of the two calibration modes will be used.

The shutter and filter commands cause those devices to advance to the commanded position.

The exposure time command determines the length of the exposure time following the exposure activate command.

TABLE 12.1

COMMAND LIST
(8 Command Bytes)

COMMAND	BITS
POWER SELECT	3
MODE SELECT	4
SHUTTER	3
CALIBRATION	1
FILTER	12
EXPOSURE TIME	18
SPARE	23
TOTAL	64

Table 12.2 gives the data list for the Planetary Camera and the number of bits. The data output follows the standard format. First the command list is echoed. Then the status monitor samples are read out, followed by calibration reference samples.

TABLE 12.2

DATA LIST
(24 Data Bytes)

	BITS
COMMAND LIST ECHO	64
STATUS MONITOR SAMPLES (8 Bits Each)	56
CALIBRATION REFERENCE SAMPLES (12 Bits Each)	60
SPARE	4
END-OF-TRANSFER CODE	8
TOTAL	192

The readout rate of the CCD array is limited to the 100 KHZ range because of the small conductors required to minimize thermal conductivity.

At this time, no system for formatting and sample rates has been established firmly by NASA.

One system proposed for the SI Command and Data Handling is described in the "Report on Large Space Telescope Scientific Instrument Command and Data Handling Study," Goddard Space Flight Center (X-604-75-224).

13.0 DESIGN VERIFICATION PLAN

The present protoflite approach to hardware development delays the availability of complete instrument verification to the F.P.A. level of SI testing. To improve the system performance predictions we have inserted into the verification plan, testing and analyses at the breadboard level of all functioning subsystems. Specifically, qual level tests will be conducted on the electronic camera and the filter assembly including its supporting electronics. Analytical and physical models of the thermal control system will be verified at the SI and F.P.A. assembly level with complete environmental tests. Structural testing is not planned in the development phase, since it is expected that the design safety factors utilized negate this requirement. Our recommendation for the optical system is to verify the design with an SR&T effort but since this may not come about, we have planned to completely breadboard and test the optical components of the reimaging optics.

Per the GSFC LST/SI plan, we are providing a fully debugged and checked out SI unit to GSFC. We plan to conduct a partial acceptance type test in a simulated environment on the instrument prior to shipment in test facilities available at Itek. Final acceptance and qualification will be at GSFC with all instruments operating in concert, mounted in the E.M.F.P.A., and tested with an optical simulator and an SSM simulator supplied by GSFC.

Table 13.1 summarizes the camera design verification plan.

TABLE 13.1

DESIGN VERIFICATION PLAN

SUB ASSEMBLY LEVEL	BREADBOARD/ENG. MODEL	FLIGHT MODEL
. ELECTRONIC CAMERA (SEC OR CCD)	QUAL LEVEL TESTS (SE)	PERFORMANCE TESTS (A)
. IMAGING OPTICS	PERFORMANCE TESTS (A)	PERFORMANCE TESTS (A)
. FILTER ASSEMBLY	QUAL LEVEL TESTS (SE)	PERFORMANCE TESTS (A)
..THERMAL CONTROLS	THERMAL MODEL TESTED (SE) IN SIMULATED ENVIRONMENT	———
. SYSTEM	———	PERFORMANCE TEST (A) PRE-ACCEPT. TEST (SE)
. SI/FPA		
THERMAL/STRUCTURAL MODELS	COMP. ENV. TEST (SE)	
FLIGHT INSTRUMENTS		PROTOFLIGHT TESTS

SE - SIMULATED ENVIRONMENT

A - AMBIENT

14.0 SUPPORT EQUIPMENT REQUIREMENTS

Support equipment is required at the various sub assembly levels in the factory build-up and test process for the camera systems. With the projected procurement of the electronic camera with the instrument, a complete test set including an SI interface assembly, T&C console and the optics bench and target simulators is required. Conduct of subsystem tests will require a thermal-vacuum test facility to evaluate the camera and thermal controls performance in a simulated space environment. At the system level tests, an F.P.A. interface simulator which provides optical targets for the camera system is required. This simulator and the SI will be installed in a thermal-vacuum facility and operated from an SSM simulator/T&C console which:

a. Provides commands and controls to the SI

b. Records, stores and presents the output of the camera system for evaluation of instrument performance and diagnosis of internal failures

This assembly can later be upgraded for delivery to GSFC, on the integration site for on-site trouble-shooting and instrument calibration.

Table 14.1 summarizes the support equipment requirements.

TABLE 14.1

SUPPORT EQUIPMENT REQUIREMENTS

SUB-ASSEMBLY LEVEL	REQUIREMENTS
Electronic Camera	Test and Checkout Bench Console Optical Bench and SI Interface Assembly Target Simulator
Imaging Optics	Optical Bench and Test Optics
Filter Assembly	Test and Checkout Bench Console Environmental Test Facility
Thermal Model	Environmental Test Facility
System	SSM Simulator/Test and Checkout Console FPA Interface Simulator Environmental Test Facility

Figure 14.1 shows a simple test fixture that could be used as part of the FPA interface simulator in verifying the performance of the camera. It uses a simple set of optics adjustable on slides to simulate the OTA image one point at a time. A star can be simulated at any point in the field by adjusting each of the five adjustments to precomputed values for that particular field point. In the simplest form, the optics would be refractive, and the full spectral range of the cameras would be tested quasi-monochromatically, using the camera filters and computing the focus adjustment for the simulator optics separately for each center wavelength.

The fixture contains registration fittings for the instrument module that are identical to those on the OTA.

FIGURE 14.1

TEST FIXTURE FOR PLANETARY CAMERA

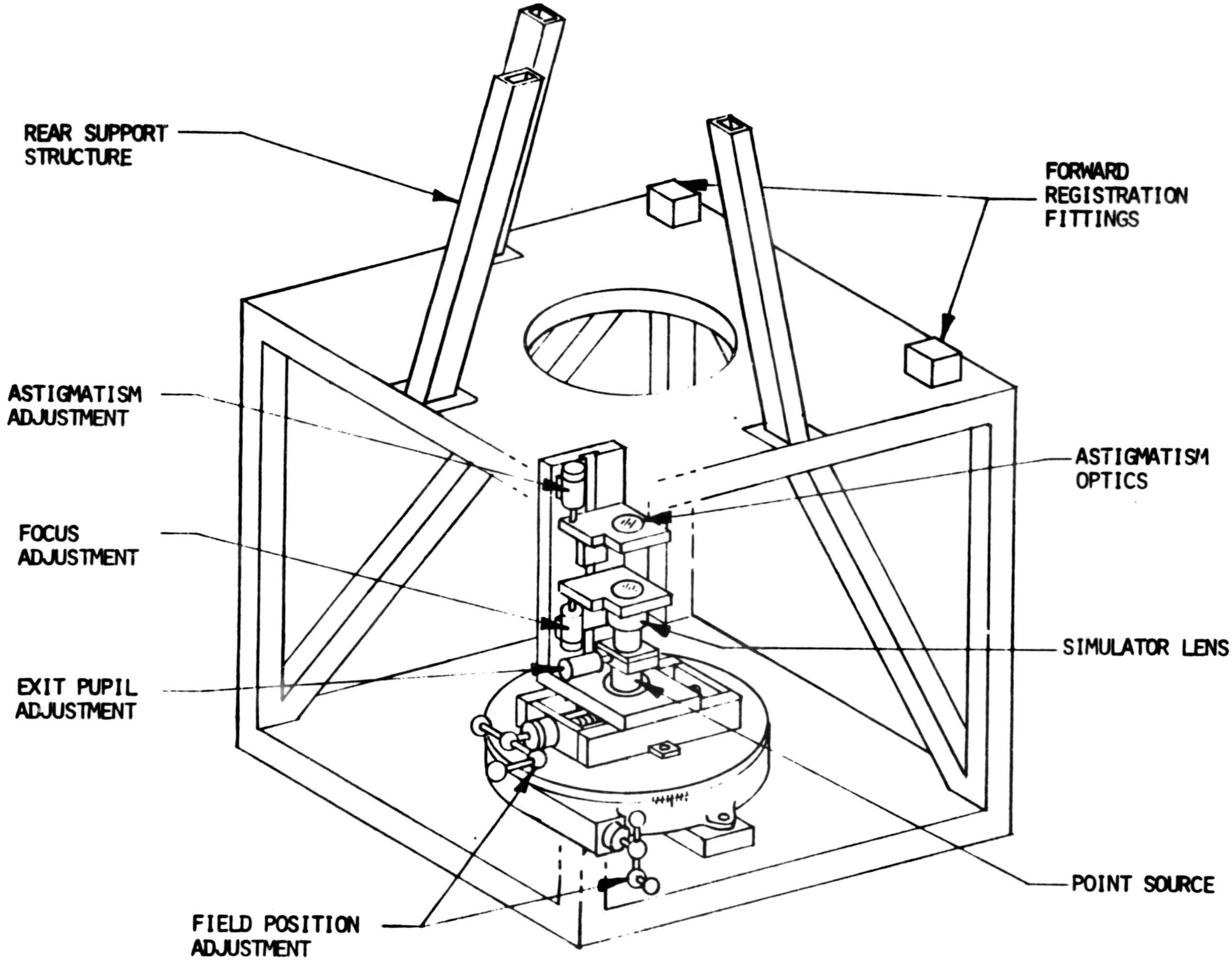

NASA—MSFC—C